European Journal of Pharmaceutical Sciences 190 (2023) 106580

Contents lists available at ScienceDirect

European Journal of Pharmaceutical Sciences

journal homepage: www.elsevier.com/locate/ejps

TAT decorated siRNA polyplexes for inhalation delivery in anti-asthma therapy

Salvatore Emanuele Drago [a], Marta Cabibbo [a], Emanuela Fabiola Craparo [a], Gennara Cavallaro [a,b,c,*]

[a] Lab of Biocompatible Polymers, Dipartimento di Scienze e Tecnologie Biologiche Chimiche e Farmaceutiche (STEBICEF), Università degli Studi di Palermo, Via Archirafi 32, Palermo 90123, Italy
[b] Consorzio Interuniversitario Nazionale per la Scienza e Tecnologia dei Materiali (INSTM) of Palermo, Palermo, Italy
[c] Advanced Technology and Network Center (ATeN Center), Università di Palermo, Palermo 90133, Italy

ARTICLE INFO

Keywords:
siRNA, STAT6
Polyaspartamide
TAT
Polyamine
Polyplexes
Asthma

ABSTRACT

In this work, a novel protonable copolymer was designed to deliver siRNA through the inhalation route, as an innovative formulation for the management of asthma. This polycation was synthesized by derivatization of α,β-poly(N-2-hydroxyethyl)D,L-aspartamide (PHEA) first with 1,2-Bis(3-aminopropylamino)ethane (bAPAE) and then with a proper amount of maleimide terminated poly(ethylene glycol) (PEG-MLB), with the aim to increase the superficial hydrophilicity of the system, allowing the diffusion trough the mucus layer. Once the complexation ability of the copolymer has been evaluated, obtaining nanosized polyplexes, polyplexes were functionalized on the surface with a thiolated TAT peptide, a cell-penetrating peptide (CPP), exploiting a thiol-ene reaction. TAT decorated polyplexes result to be highly cytocompatible and able to retain the siRNA with a suitable complexation weight ratio during the diffusion process through the mucus. Despite polyplexes establish weak bonds with the mucin chains, these can diffuse efficiently through the mucin layer and therefore potentially able to reach the bronchial epithelium. Furthermore, through cellular uptake studies, it was possible to observe how the obtained polyplexes penetrate effectively in the cytoplasm of bronchial epithelial cells, where they can reduce IL-8 gene expression, after LPS exposure. In the end, in order to obtain a formulation administrable as an inhalable dry powder, polyplexes were encapsulated in mannitol-based microparticles, by spray freeze drying, obtaining highly porous particles with proper technological characteristics that make them potentially administrable by inhalation route.

1. Introduction

Asthma affects about 300 million individuals around the world, representing a serious health problem that affects all age groups, with a constantly increasing incidence in many countries (Global Initiative for Asthma - GINA, 2023).

The fundamental mechanism for the development and progression of the disease, regardless of clinical severity, is represented by the inflammatory process (Williams and Jose, 2000), which mainly involves eosinophils, neutrophils, $CD4^+$ T lymphocytes and mast cells (Kay, 2005).

The inflammatory process is generally limited to the conducting airways, but consequently to disease progression, the inflammatory infiltrates also reach the small airways and alveoli (Kraft et al., 1999).

Many possible factors can trigger the asthmatic response; after the interaction of these factors with immune cells, a molecular cascade begins which leads to an increase in the production and release of inflammation mediators (IL- 3, IL-4, IL-5, IL-6, IL-9, IL-13 ed GM-CSF) (Ying et al., 1997; Kay, 2006; Ryu et al., 2006).

The long-term goals in the management of asthma concern both the control of symptoms, reducing the impact of the disease on the patient, and the reduction of damage of airways that occurs with the progression of the disease (Paggiaro, 2019).

In this regard, the administration of drugs by inhalation route offers the possibility of a therapy targeted for lung diseases, reducing systemic exposure to the drug, systemic side effects and therapy costs.

* Corresponding author at: Lab of Biocompatible Polymers, Dipartimento di Scienze e Tecnologie Biologiche Chimiche e Farmaceutiche (STEBICEF), Università degli Studi di Palermo, *Via* Archirafi 32, Palermo 90123, Italy.
E-mail address: gennara.cavallaro@unipa.it (G. Cavallaro).

https://doi.org/10.1016/j.ejps.2023.106580
Received 22 December 2022; Received in revised form 20 July 2023; Accepted 8 September 2023
Available online 16 September 2023
0928-0987/© 2023 Published by Elsevier B.V. This is an open access article under the CC BY-NC-ND license (http://creativecommons.org/licenses/by-nc-nd/4.0/).

To date, drugs approved for the treatment of asthma include bronchodilators (β2 agonists and anticholinergics) and corticosteroids. These latter, although represent the most effective therapy for asthma, involve a series of side effects (Heffler et al., 2018; Scherholz et al., 2019; d'Ancona et al., 2020; Jackson and Bacharier, 2021) and are ineffective in subjects resistant to steroid treatment (Chung et al., 2014; Beck et al., 2009).

Regarding the innovative monoclonal antibody Omalizumab, although it is effective in the management of uncontrolled asthma in patients with allergic asthma from moderate to severe persistent (Sulaiman et al., 2016), its use has been associated with anaphylaxis and atherothrombotic events such as myocardial infarction and stroke (Ali and Hartzema, 2012).

In the particular case of asthma, where the inflammatory cascade includes a large number of proteins, a possible innovative alternative is represented by *small interfering* RNA (siRNA) (Gorabi et al., 2020), small double-stranded RNA able to induce the degradation of a specific mRNA (Cavallaro et al., 2017a), reducing thus the expression of a specific gene.

Among the possible targets of siRNAs involved in the pathogenesis of asthma identified to date, some genes encode for cytokines (IL-4, IL-5, IL-13) (Koli et al., 2014; Park et al., 2016), for the chemokine receptor (CCR3), for the spleen tyrosine kinase (SYK) (Tabeling et al., 2017), for signal transducers and activators of transcription such as STAT1, STAT5b, STAT6 (Healey et al., 2013; Zhu et al., 2013), GATA3 and NF_kB (nuclear factor $_kB$) (Li et al., 2016).

Compared to traditional drugs, siRNAs show superior therapeutic effects due to their high selectivity and potency, as well as they can be designed to provide personalized therapy (Daka and Peer, 2012; Singh and Peer, 2016).

However, it is known that to exploit the potential of this genetic material, the use of particular vectors able to convey it to the site of action is needed (Cavallaro et al., 2017a; Park et al., 2016). These vectors not only increase the stability of nucleic acids against enzymatic degradation by nucleases but, by neutralizing their negative charge, they also allow cell internalization. Among the various existing vectors, polymeric materials have numerous advantages, as they can load large quantities of genetic material and can be chemically derivatized to obtain systems headed towards particular target tissues (David et al., 2010; Cooper and Putnam, 2016). However, any side effects can be associated to the components of the polyplexes (polication, siRNA or both). In particular, many of these effects are related to increased charge density, which is predominantly associated with an excess of polycation rather than the material. These effects can be avoided by using low-Mw polymers with low charge density or by shielding the charge through surface engineering, such as conjugation with hydrophilic polymers, which represent a standard method to hinder nonspecific interaction with proteins and capture by the mononuclear phagocyte system (Ballarín-González and Howard, 2012).

Beyond these considerations, for the design of an inhalable formulation, it is also necessary to take into account also the main barriers that hinder inhaled particles.

The first barrier that is interposed between the inhaled particles and their site of action is the mucus layer (He et al., 2019) that lines the airways; the latter contains secreted glycoproteins, called mucins, which form a network able to trap particles (García-Díaz et al., 2018).

Another barrier to consider is the membrane of the epithelial cells of the airways, as these cells are characterized by a low endocytotic efficiency across the apical membrane and by tight intercellular junctions that prevent the entry of substances (d'Angelo et al., 2014).

In light of these considerations, the aim of the present experimental work was to realize a novel gene delivery system designed to deliver siRNA through the inhalation route, as an innovative formulation for the management of asthma.

In particular, as starting material for the realization of the polymer carrier, we have chosen to use the α, β-poly-N-2-hydroxyethyl-DL-aspartamide (PHEA) derivatized with 1,2-Bis(3-aminopropylamino) ethane (bAPAE) (PHEA-g-bAPAE) already synthesized by us previously (Craparo et al., 2020), as it has been shown to have excellent complexing abilities, to be highly cytocompatible towards the target site and to be able to transfect the cells of the bronchial epithelium.

In view of an administration by the inhalation route, the PHEA-g-bAPAE was also derivatized with a proper amount of poly(ethylene glycol) (PEG), to increase the superficial hydrophilicity of the system, reducing interactions with the protein chains of the mucin, allowing the diffusion trough the mucus layer (Dave et al., 2021; Murgia et al., 2018).

Therefore, polyplexes were prepared using a siRNA that silences the expression of STAT6 (Darcan-Nicolaisen et al., 2009; Rippmann et al., 2005), as it is one of the most important transcription factors that initiates an asthmatic attack (Georas et al., 2021; Gour and Wills-Karp, 2015), for example, inducing the release of IL-8 from human bronchial epithelium cells (Tomita et al., 2012; Charrad et al., 2017), in response to stimulation by others inflammation mediators (StříŽ et al., 1999; Mullings et al., 2001).

Subsequently, once the best conditions for the formation of polyplexes have been established, polyplexes were functionalized on the surface with TAT peptide, a cell-penetrating peptide (CPP) already known for its ability to increase the uptake in the cells of the bronchial epithelium (Kubczak et al., 2021), exploiting a thiol-ene reaction. Therefore, the ability of these polyplexes to diffuse through the mucus layer and to be internalized by the cells of the bronchial epithelium, as well as their gene silencing activity was evaluated.

Finally, as a proof of concepts, to obtain a formulation administrable as a dry powder that allows the deposition in the deep airways, polyplexes have been encapsulated within water-soluble porous microparticles using the spray-freeze-drying technique.

2. Materials and methods

2.1. Materials

Bis (4-nitrophenyl) carbonate (BNPC), N, N'-dimethylformamide anhydrous (a-DMF), 1,2-Bis (3-aminopropylamino) ethane (bAPAE), dichloromethane, acetone, diethyl ether, 2,4,6 -trinitrobenzene sulfonic acid (TNBS), agarose, ethidium bromide, mucin from pig stomach, acetone, mannitol, Poly (ethylene oxide) standards, Dulbecco's phosphate buffer saline (DPBS), NaOH, HEPES, MES, NaCl, Ester N 4-maleimidobutyric acid hydroxysuccinimide (MLB-NHS), amino-PEG-carboxylic acid ($H2N\text{-}PEG_{2000}\text{-}OCH_2\text{-}COOH$), HIV-1 $TAT_{(47\text{-}57)}$ peptide (Tyr-Gly-Arg-Lys -Lys-Arg-Arg-Gln-Arg-Arg-Arg), N-hydroxysuccinimide ester of 3- (2-pyridyldithium) propionic acid, 1,4-dithiothreitol, acetonitrile, were purchased from Sigma-Aldrich (Milan, Italy).

HCl, Diethylamine (DEA), triethylamine (TEA), were purchased from Fluka (Italy).

All reagents used are analytical grade.

The duplex siRNA and duplex siRNA-Cy5 were purchased from Biomers.net (Ulm, Germany). The sequences (5′→3 ') are: CAGUUC CGCCACUUGCCAA (sense), UUGGCAAUGGCGGAACUG (antisense).

α, β-poly (N-2-hydroxyethyl) -D, L-aspartamide (PHEA) was synthesized by reaction of polysuccinimide (PSI) with ethanolamine in DMF solution and purified according to the procedure reported (Giammona et al., 1987). The spectroscopic data are in agreement with the attributed structure.

^{1}H NMR (300 MHz, D2O, 25 °C, TMS): δ 2.71 (m, 2H PHEA, —COCHC**H$_2$**CONH—), δ 3.24 (m, 2H PHEA, —NHC**H$_2$**CH$_2$O—), δ 3.55 (m, 2H PHEA, —NHCH$_2$C**H$_2$**OH), δ 4.59 [m, 1H PHEA, —NHC**H**(CO)CH$_2$—].

2.2. Cell culture

Human bronchial epithelial cells (16-HBE) were furnished by Istituto Zoo-profilattico of Lombardia and Emilia Romagna. 16-HBE cells were maintained in a humidified atmosphere of 5 % CO_2 in air at 37 °C,

cultured as adherent monolayers in Dulbecco's Modified Eagle's medium (DMEM) (EuroClone), supplemented with 10 % fetal bovine serum (FBS) (Gibco), 2 mM l-glutamine (EuroClone), 100 U/mL penicillin, 100 g/mL streptomycin, and 0.6 g/mL amphotericin B (Sigma–Aldrich, Milan, Italy).

2.3. Synthesis of the PHEA-g-bAPAE graft copolymer

Derivatization of PHEA with 1,2-Bis (3-aminopropylamino)ethane (bAPAE) was performed using Bis (4-nitrophenyl) carbonate (BNPC) as coupling agent. 200 mg of PHEA (corresponding to 1.26 mmol of repeating units) were solubilized in 4 mL of a-DMF; after complete solubilization, 230 mg of solid BNPC were added. The solution was kept under continuous stirring at 40 °C for 4 h. At the same time, 922.71 μL of bAPAE were mixed with 7 mL of a-DMF. After the activation time, the resulting polymer solution was added dropwise and slowly to the bAPAE solution. The reaction was kept under continuous stirring at 25 °C for 20 h. The quantities of each reagent were determined considering the following stoichiometric ratios: R1 = (mmol of BNFC / mmol of functionalizable UR of PHEA) = 0.6 and R2 = (mmol of bAPAE / mmol of functionalizable UR of PHEA) = 4.

After the reaction time, the polymer was isolated from the reaction mixture by precipitation in a 2: 1 v / v diethyl ether/dichloromethane mixture and the supernatant was removed by centrifugation at 4 °C for 8 min, at 9800 rpm. The solid product obtained was washed with acetone until the pH of the acetone waters mixture (1:1) was neutral. Then, the obtained product was dried under vacuum. The solid residue was solubilized in double distilled water and the solution was purified by exhaustive dialysis (SpectraPor Dialysis Tubing, at MWCO 25 kDa), two days against basic water (NaOH) and other three days against double distilled water. After lyophilization, the PHEA-g-bAPAE copolymer was obtained with a yield of 80 % by weight to the initial PHEA amount.

^{1}H NMR (300 MHz, D_2O pD 5, 25 °C, TMS): δ 1.70 - 2.20 (m, $4H_{bAPAE}$, —NHCH$_2$C**H$_2$**CH$_2$NHCH$_2$CH$_2$NHCH$_2$C**H$_2$**CH$_2$NH—), δ 2.73 (m, $2H_{PHEA}$, —COCHC**H$_2$**CONH—), δ 3,12 (m, $8H_{bAPAE}$, —NHC**H$_2$**CH$_2$ C**H$_2$**NHCH$_2$CH$_2$NHC**H$_2$**CH$_2$C**H$_2$**NH$_2$), δ 3.23 (m, $2H_{PHEA}$, —NHC**H$_2$** CH$_2$O—), 3,38 (m, $4H_{bAPAE}$, —CONHC**H$_2$**CH$_2$—, —CH$_2$CH$_2$C**H$_2$**NH$_2$), δ3.54 (m, $2H_{PHEA}$,—NHCH$_2$C**H$_2$**OH), δ 3.60 (m, $4H_{PEG}$,—[OC**H$_2$**-C**H$_2$**O]$_{44}$-), δ 4.02 (m, $2H_{PHEA}$, —NHCH$_2$C**H$_2$**OCO—), δ 4.62 (m, $1H_{PHEA}$, -NHC**H**(CO)CH$_2$-).

The amine content was also determined by the TNBS colorimetric assay (Cavallaro et al., 2017b), as follow: 950 ml of PHEA-bAPAE (0.25 mg/ml) in $Na_2B_4O_7{\cdot}H_2O$ 0.1 M, pH 9.3 were mixed with 50 ml of 0.03 M TNBSA solution. After 120 min incubation, absorbance at l 500 nm was measured and compared with that estimated for the reaction of H_2N-PEG—OCH_3 (—NH_2 in the range between 0.01 and 0.001 mmol/ml) with TNBSA.

2.4. Synthesis of the MLB-PEG-COOH polymer

The synthesis of the MLB-PEG-COOH polymer was carried out by exploiting the reactivity of the terminal amino group of amino-PEG-acid (NH_2-PEG-COOH) towards the succinimide ester of 4-Maleimidobutyric acid (MLB-NHS). 100 mg of NH_2-PEG-COOH (0.0476 mmol) were solubilized in 600 μL of DPBS and mixed with 16 mg of MLB-NHS (0.0571 mmol), previously solubilized in 1.4 mL of a DPBS: DMSO mixture (86:14 v / v), considering the stoichiometric ratio: R1 = (mmol of MLB-NHS / mmol of PEG) = 1.2.

The reaction was maintained under continuous stirring at 25 °C overnight and subsequently, the reaction product was purified by size exclusion chromatography, using a Sephadex G15 as the stationary phase and bidistilled water as the mobile phase. The collected fractions are, therefore, frozen and freeze-dried, obtaining a yield of 95 % by weight with respect to the total amount of the reagents used.

^{1}H NMR (300 MHz, D_2O 25 °C, TMS): δ 1.8 ($2H_{MLB}$, —CH$_2$C**H$_2$**CH$_2$—COOH), δ 2.2 ($2H_{MLB}$, —CH$_2$CH$_2$C**H$_2$**—COOH), δ 3.70 (m, $4H_{PEG}$, - [OC**H$_2$**C**H$_2$**O]$_{44}$-), δ 6.8 (m, $2H_{MLB}$,-CO—C**H**=C**H**—CO).

2.5. Synthesis of the PHEA-g-bAPAE-PEG-MLB copolymer

The derivatization of PHEA-g-bAPAE with MLB-PEG-COOH was performed using 1-ethyl-3- (dimethylaminopropyl) carbodiimide chloride (EDC · HCl) and N-hydroxysuccinimide (NHS) as conjugating agents.

50 mg of MLB-PEG-COOH were solubilized in 300 μL of 0.1 M MES (2- (N-morpholino) ethanesulfonic acid) buffer, 0.5 M NaCl, pH 6.0. Subsequently, 3.84 mg of EDC · HCl and 2.83 mg of NHS previously solubilized in 100 μL of 0.1 M MES buffer, 0.5 M NaCl, pH 6.0 were added.

The mixture was kept under continuous stirring for 4 h at 25 °C; at the same time, 100 mg of PHEA-g-bAPAE were solubilized in 1 mL of DPBS, adjusting the pH around 7 using 30 % HCl.

After the activation time of 4 h, the PEG solution was slowly added under continuous stirring to the solution of PHEA-g-bAPAE; the obtained mixture was kept at 25 °C overnight and finally, it was purified by exhaustive dialysis using acidic water (pH 5) as the exchange medium.

The quantities of each reagent were determined considering the following stoichiometric ratios: R1 = (mmol of EDC/mmol PEG) = 1.1, R2 = (mmol of NHS/mmol PEG) = 1.1, R3 = (mmol of PEG/mmol of UR of PHEA-g-bAPAE) = 0.05.

After lyophilization, the PHEA-g-bAPAE-PEG-MLB copolymer was obtained with a yield of 70 % by weight with respect to the sum of the initial quantities of PHEA-g-bAPAE and MLB-PEG-COOH.

^{1}H NMR (300 MHz, D_2O pD 5, 25 °C, TMS): δ 1.70-2.20 (m, $4H_{bAPAE}$, —NHCH$_2$C**H$_2$**CH$_2$NHCH$_2$CH$_2$NHCH$_2$C**H$_2$**CH$_2$NH—), δ 2.73 (m, $2H_{PHEA}$, —COCHC**H$_2$**CONH—), δ 3.12 (m, $8H_{bAPAE}$, —NHC**H$_2$**CH$_2$C**H$_2$**NHCH$_2$ CH$_2$NHC**H$_2$**CH$_2$C**H$_2$**NH$_2$), δ 3.23 (m, $2H_{PHEA}$, —NHC**H$_2$**CH$_2$O—), 3,38 (m, $4H_{bAPAE}$, —CONHC**H$_2$**CH$_2$—, —CH$_2$CH$_2$C**H$_2$**NH$_2$), δ3.54 (m, $2H_{PHEA}$, —NHCH$_2$C**H$_2$**OH), δ 3.60 (m, $4H_{PEG}$, -[OC**H$_2$**C**H$_2$**O]$_{44}$-), δ 4.02 (m, $2H_{PHEA}$, —NHCH$_2$C**H$_2$**OCO—), δ 4.62 (m, $1H_{PHEA}$, —NHC**H**(CO) CH$_2$—).

2.6. Functionalization of TAT peptide with the succinimide ester of 3- (2-pyridyldithium) propionic acid (SPDP)

10 mg of $TAT_{(47\text{-}57)}$ peptide (corresponding to 6.41 μmoles) were solubilized in 1 mL of 50 mM sodium phosphate buffer, 0.15 M NaCl, pH 7.2 and subsequently 442 μL of a 20 mM SPSP solution were added in DMSO (corresponding to 8.77 μmoles).

The reaction mixture was kept at 25 °C overnight; subsequently, the mixture was diluted with 1 mL of DMSO and purified by exhaustive dialysis (SpectraPor Dialysis Tubing, at MWCO 100–500 Da) using double distilled water as the exchange medium.

After lyophilization, the TAT-SPDP conjugate was obtained with a yield of 80 % by weight with respect to the initial quantity of TAT.

The product obtained was characterized by FT-IR spectroscopy and by HPLC analysis using a Phenomenex Luna C18 column; the chromatographic separation was carried out using gradient elution with 2 solvents: H_2O + 0.1 % TFA (solvent A) and ACN + 0.1 % TFA (solvent B) with a flow rate of 1 mL min^{-1}. The initial ratio between the mobile phases A: B was 90:10 and the amount of solvent B was gradually increased until 100 % of B in 60 min. ^{1}H NMR (300 MHz, D_2O:DMSO, 25 °C, TMS): δ 1.4 ($4H_{Lys}$, C**H$_2$**—CH$_2$—CH$_2$—NH$_2$), δ 1.55–1.7 ($20H_{Arg}$ CO—CH—C**H$_2$**—C**H$_2$**—; $8H_{Lys}$ CH—C**H$_2$**—C**H$_2$**; $2H_{Gln}$ C**H$_2$**—CO—N**H$_2$**). δ -2.25 ($2H_{Gln}$ .C**H$_2$**—CH$_2$—CO—NH$_2$), δ 2.86 ($4H_{Lys}$ CH$_2$—C**H$_2$**—NH$_2$), δ 3.1 ($10H_{Arg}$—NH—C**H$_2$**—CH$_2$—$_{Tyr}$—C**H**—CH$_2$—C—), δ 4.2 ($2H_{Gly}$ CO-C**H$_2$**—NH—), δ 4.2 ($5H_{Arg}$—NH—C**H**—CO—;$2H_{Lys}$—NH—C**H**—CO—; $1H_{Gln}$—NH—C**H**—CO—), δ 6.8 ($2H_{Tyr}$ C**H**—C—C**H**—), δ 7.0 ($2H_{Tyr}$ C**H**—C—C**H**—), δ 7.2 ($1H_{SPDP}$—N—CH—C**H**—CH—CH), δ 7.7 ($2H_{SPDP}$—N—CH—CH—C**H**—C**H**), δ 8.3 ($1H_{SPDP}$—N—C**H**—CH—CH—CH).

2.7. Deprotection of the thiol group in the TAT-SPDP conjugate

Deprotection of the thiol group introduced into the TAT peptide was carried out using dithiothreitol (DTT) as a reducing agent.

7.5 mg of TAT-SPDP were solubilized in 500 μL of 0.1 M sodium acetate buffer, 0.1 M NaCl, at pH 4.5 and mixed with 325 μL of 20 mg mL^{-1} DTT in 0.1 M sodium acetate, 0.1 M NaCl, pH 4.5. The mixture was kept at 25 °C for one hour and was subsequently purified by exhaustive dialysis (SpectraPor Dialysis Tubing, at MWCO 100–500 Da) using acidic water (pH 5) as the exchange medium, protected from light.

The product was obtained with a yield higher than 95 % and was stored in an inert atmosphere at -20 °C.

The deprotection was confirmed by a colorimetric assay for the quantitative analysis of thiols (Ellman's assay).

2.8. Size exclusion chromatography

Weight-average molecular weight (Mw), polydispersity (Mw/Mn), of copolymers was determined by a size exclusion chromatography (SEC) analysis, performed using PolySep-GFC-P4000 columns (PHENOMENEX) connected to an Agilent 1260 Infinity Multi-Detector GPC/SEC system (Santa Clara, United States), equipped with a refractive index detector and a light scattering detector.

Analyses were performed with buffer citrate/phosphate 0.15M+ 0.1MNaCl pH 5 as eluent with a flow of 1 mL min^{-1}, using poly(ethylene oxide) standard (40 kDa) as standard. The column temperature was set at 30 °C.

2.9. Complexation study

Complexation studies were carried out by gel retard assay.

The polyplexes were formed by adding a copolymer dispersion (10 μL), with different concentrations, to the same volume of siRNA solution (10 μL) with a fixed concentration, to obtain different polymer / siRNA weight ratios (R); the mixture was mixed gently by pipetting and incubated 30 min at room temperature before each analysis.

The polyplexes were formed in 10 mM HEPES nuclease free buffer, at pH 7.4, containing 5 % glucose (w / v). The siRNA concentration used was 0.1 mg mL^{-1} and the polymer / siRNA weight ratios (R) were: 0, 1, 2, 2.5, 3, 3.5, 4, 5.

15 μL of each sample were then loaded onto a 1.5 % agarose gel containing 70 μL of ethidium bromide and run at 100 V in tris acetate / EDTA buffer (TAE) at pH 8 for 20 min. The gels were then visualized *via* a UV transilluminator and photographed using a digital camera.

2.10. Preparation of TAT coated nanocomplexes

The polyplexes (200μL) were prepared by mixing 100 μL of siRNA solution (0.2 mg mL^{-1}) and 100 μL of polymer dispersion, in order to obtain polymer / siRNA weight ratios (R) equal to 10; the mixture was mixed gently by pipetting and incubated for 30 min.

Subsequently, a double amount of TAT peptide (50 μL, 60.5 nmol) with respect to that necessary to functionalize all the PEG chains (30.25 nmol) was added; the mixture was mixed by gently pipetting and incubated for 2 h at 37 °C.

The amount of conjugated peptide was subsequently determined by the difference between the total amount of the added peptide and the amount of unreacted residual peptide, determined by the colorimetric assay for the quantitative analysis of thiols (Ellman's assay).

2.11. Stability to polyanionic exchange of polyplexes in the presence of mucins

The stability of the polyplexes to polyanion exchange was determined after incubation of the polyplexes with mucin dispersion. The polyplexes were prepared as previously described, in order to obtain polymer / siRNA weight ratios (R) equal to 5 and 10, and adding subsequently 10 μL of TAT 150 μM or 10 μL of 10 mM Hepes; after 2 h, the resulting polyplexes (30 μL) were mixed with 5 μL of mucin dispersion (7 mg mL^{-1}), in order to have a final mucin concentration of 1 mg mL^{-1}, and the samples were been incubated at room temperature for 5 h. Gel electrophoresis was then performed as described in the complexation study.

2.12. Dynamic light scattering (DLS) measurements

For DLS studies, the polyplexes were formed in 10 mM Hepes nuclease free buffer, at pH 7.4, obtaining a polymer / siRNA (R) weight ratio of 10, using a concentration of siRNA equal to 0.2 mg mL^{-1}. After 30 min of incubation, the obtained polyplexes (40 μL) were mixed with the TAT peptide (20 μL 300 μM) or with 10 mM Hepes and were incubated for 2 h.

The DLS measurement was performed on 60 μL of sample at 25 °C with a Malvern Zetasizer NanoZS equipped with a 633 nm laser with a fixed scattering angle of 173°, using Dispersion Technology Software 7.02.

Subsequently, for the zeta potential, the polyplexes were diluted with nuclease free water up to 900 μL before measurement. Zeta potential measurements were performed by aqueous electrophoresis measurements, recorded at 25 °C using the same apparatus as the DLS. The zeta potential (mV) values were calculated from electrophoretic mobility using the Smoluchowski relation.

2.13. Evaluation of polyplexes-mucin interactions

The evaluation of the possible interactions between polyplexes and mucins was carried out by turbidimetric assay. 40 μL of polyplexes were prepared by mixing equal volumes (20 μL) of siRNA (0.1 mg mL^{-1}) and copolymer solutions, obtaining a polymer / siRNA weight ratio (R) equal to 10.

After 30 min of incubation, the obtained polyplexes (40 μL) were mixed with the TAT peptide (20 μL, 150 μM) or with 10 mM Hepes and incubated for 2 h.

Subsequently, 60 μL of mucin dispersion (2 mg mL^{-1} in 10 mM Hepes buffer pH 7.4) were added. After incubation at 37 °C, turbidity was measured every 50 min up to approximately 6 h. The absorbance at λ of 500 nm was recorded by the microplate reader (Multiskan Ex, Thermo Labsystems, Finland).

Similarly, the absorbance at λ of 500 nm was recorded for polyplexes mixed with 60 μL of buffer, in order to subtract the absorbance owing to scattering phenomena of the polyplexes, and for mucin dispersion (1 mg mL^{-1} in 10 mM Hepes buffer pH 7.4).

Results were expressed as % of trasmittance [(Abs500 mucins / Abs500 samples) × 100].

2.14. Evaluation of the mucopenetrant ability of polyplexes

To evaluate the ability of polyplexes to diffuse through a mucus layer, a custom-made system was used, consisting of a donor and an acceptor (Grießinger et al., 2015).

The polyplexes were formed by mixing equal volumes (125 μL) of siRNA-Cy5 (0.105 mg mL^{-1}) and copolymer, obtaining a polymer / siRNA weight ratio (R) equal to 10. After 30 min of incubation, the obtained polyplexes (250 μL) were mixed with the TAT peptide (50 μL 375 μM) and incubated for 2 h.

For the realization of the system, inserts for cell plates (Scaffdex, CellCrownTM48) were used, equipped with a hydrophilic polypropylene membrane with 0.45 μm pores.

Subsequently, the inserts were placed in 24-well plates, containing 1 mL of DPBS, using plastic support so that the membrane is in contact with the surface of the liquid.

100 μL of a mucin dispersion 1 mg mL^{-1} were placed on the

membrane and then the previously obtained polyplexes (300 μL) have been deposited on the mucin layer.

The system was then placed in an incubator at 37 °C under continuous stirring (50 rpm). The fluorescence intensity at λ of 665 nm of the acceptor compartment was measured every hour up to 5 h. The emission spectra were recorded by a spectrofluorimeter (Shimadzu RF-5301PC) (Milan, Italy) at the excitation wavelength of 600 nm.

For comparison, the same experiment was repeated in the absence of mucin.

2.15. Cell viability test

Cell viability was evaluated by an MTS assay on 16-HBE cells, using a commercially available kit (cell proliferation test with an aqueous solution of Titer 96, Promega cell solution) containing 3- (4,5-dimethylthiazol-2 -yl) -5- (3-carboxymethoxyphenyl) -2- (4-sulfophenyl) -2H-tetrazolium (MTS) and phenazine ethosulfate. 16-HBE cells were incubated in a 96-well plate with a density of 15,000 cells per well in DMEM containing 10 % FBS. After 24 h of incubation, the medium was removed and then the cells were incubated with 200 μL per well of OPTI-MEM containing polyplexes. The polyplexes were prepared with weight ratios of 3, 5, 10 and 15, adding or not the TAT peptide and obtaining a final siRNA concentration of 200 nM.

Similarly, cells were incubated with PHEA-g-bAPAE-PEG-MLB copolymer at concentrations ranging from 0.5 mg mL^{-1} to 0.005 mg mL^{-1}.

All the reagents used were sterilized by filtration with a 220 nm cellulose acetate filter before the formation of the complexes. After 24 and 48 h of incubation, the solutions were removed and each well was washed with sterile DPBS; subsequently, the cells of each well were incubated with 100 μL of fresh DMEM and 20 μL of an MTS solution and the plates were incubated for 2 h at 37 °C.

The absorbance at 490 nm was read using a plate reader (Multiskan Ex, Thermo Labsystems, Finland). Relative cell viability (percent) was expressed as (Abs490 treated cells / Abs490 control cells) × 100, based on three experiments. Cells incubated with OPTI-MEM medium only were used as a negative control.

2.16. Cell uptake study

The cellular internalization ability of the polyplexes was evaluated by uptake studies on 16-HBE.

Cells were plated on an 8-well plate with a density of 10,000 cells per well in DMEM containing 10 % FBS. After 24 h of incubation, the medium was removed and then the cells were incubated with 200 μL per well of OPTI-MEM containing polyplexes PHEA-g-bAPAE-PEG-MLB / siRNA-Cy5, obtained with a weight ratio equal to 10, adding or not the TAT peptide and obtaining a final siRNA concentration of 200 nM.

After 4 or 24 h, the cells were washed with 300 μL of sterile DPBS and fixed with 4 % formaldehyde for 10 min. Subsequently, the formaldehyde solution was removed and the nuclei were stained with 100 μL of 4 ', 6-diamidino-2-phenylindole (DAPI) in DPBS at a concentration of 5 × 10–3 mg mL^{-1}. After 3 min of incubation, the DAPI solution was removed and the cells were washed three times with DPBS and observed by an Axio Vert.A1 (Zeiss) fluorescence microscope. The images were recorded using an Axio Cam MRm (Zeiss).

For the quantitative determination of cell uptake, 16-HBE cells were seeded in a 24-well plate with a density of 100,000 cells per well. After 24 h of incubation, the medium was removed and then the cells were incubated with 300 μL per well of OPTI-MEM containing polyplexes PHEA-g-bAPAE-PEG-MLB / siRNA-Cy5, obtained with a weight ratio equal to 10, adding or not the TAT peptide and obtaining a final siRNA concentration of 200 nM.

After 4 or 24 h of incubation, the cells were extensively washed with sterile DPBS and lysed in 100 μL of lysis buffer (2 % SDS, 1 % Triton X-100, in sterile DPBS). The lysates were divided into two parts: the first (75 μL) was used to measure the fluorescence intensity by a Shimadzu RF-5301PC spectrofluorophotometer (λex: 600 nm; λem: 665 nm); the second (25 μL) was used to evaluate the total amount of protein through the BCA assay. The results were expressed as the ratio of fluorescence intensity per milligram of protein.

All the reagents used were sterilized by filtration with a 220 nm cellulose acetate filter before the formation of the complexes.

2.17. Gene silencing assay

The evaluation of the gene silencing capacity was evaluated by ELISA test, using IL-8 Human

ELISA Kit kits from Life Technologies. For this study PHEA-g-bAPAE-PEG-MLB / siRNA polyplexes (130 μL) were prepared in 10 mM Hepes nuclease free buffer at pH 7.4, by mixing the same volume (65 μL) of polymer and siRNA dispersion (1 μM), obtaining a polymer / siRNA (R) weight ratio of 10. After 30 min of incubation, 9 μL of TAT dispersion in Hepes buffer (150 μM) and incubated for another 2 h and then diluted with OPTIMEM up to 650 μL.

Uncoated polyplexes were prepared in the same way, adding 9 μL of Hepes buffer instead of TAT.

16-HBE cells were plated on a 96-well plate at a cell density of 20,000 cells/well in DMEM containing 10 % FBS. After 24 h of incubation, the medium was removed and then the cells were incubated with 200 μL of a polyplexes dispersion (0.01 nmol of siRNA/ well).

After 48 h supernatant was removed and the cells were incubated with 100 μL of LPS 10 μg mL^{-1} for 24 h. After this time 50 μL of supernatant were treated following the protocol provided, while the cells were washed with DPBS and cell viability was evaluated as described for cell viability test.

The test was also repeated using a siRNA whose sequence is not active in the cellular pathway studied.

All the reagents used were sterilized by filtration with a 220 nm cellulose acetate filter before the formation of the complexes.

2.18. Preparation of microparticles by spray freeze drying technique

Microparticles containing polyplexes were prepared by atomization of a water polyplexes dispersion into liquid nitrogen under continuous stirring, using the atomizer apparatus of Nano Spray Dryer B-90 (Buchi, Milan, Italy).

PHEA-g-bAPAE-PEG-MLB / siRNA polyplexes (1 mL) were prepared in 10 mM Hepes nuclease free buffer at pH 7.4, by mixing the same volume (500 μL) of polymer (2 mg mL^{-1}) and siRNA dispersion (0.2 mg mL^{-1}), obtaining a polymer / siRNA (R) weight ratio of 10. After 30 min of incubation, 1 μL of TAT dispersion in Hepes buffer (150 μM) and incubated for another 2 h and then 50 mg of mannitol was added, obtaining mannitol concentrations equal to 5 % (% w/v); after the complete solubilization of mannitol, the mixture was filtered with 450 nm cellulose acetate filter and subsequently it was atomized into liquid nitrogen under continuous stirring. The obtained frozen droplets were quickly transferred into the chamber of a freeze dryer system.

2.19. siRNA quantification in microparticles

The quantification of siRNA content encapsulated into the microparticles, after the spray-freeze-dying process, was performed using an ethidium bromide (EtBr) exclusion assay as described elsewhere (Segura and Hubbell, 2007; Itaka et al., 2003).

According to the theoretical content of siRNA, a proper amount of microparticles was dispersed in one ml of nuclease free water to achieve a concentration of approximately 0.02 mg/ml of siRNA. 250 μl of this aqueous dispersion was mixed thoroughly with 250 μl of an EtBr aqueous solution (0.02 mg mL^{-1}), and the obtained mixture was incubated for 5 min in the dark at room temperature. Afterwards, the fluorescence of the mixture was measured at λex of 527/20 nm and λem of

585/20 nm using a Microplate reader (Multiskan Ex, Thermo Labsystems, Finland) and compared to a fresh polyplexes sample, prepared as described before, incubated with EtBr aqueous solution. The assay was performed in 96 black well plate in triplicate.

2.20. Evaluation of microparticles gene silencing capacity

The evaluation of the gene silencing capacity of microparticles was evaluated by ELISA test, using IL-8 Human ELISA Kit kits from Life Technologies. For this study, 1.36 mg of microparticles (or pure mannitol) were dispersed in 2 ml of Optimem/water mixture (85:15).

16-HBE cells were plated on a 96-well plate at a cell density of 20,000 cells/well in DMEM containing 10 % FBS. After 24 h of incubation, the medium was removed and then the cells were incubated with 200 μL of a sample dispersion (0.01 nmol of siRNA/ well).

After 48 h supernatant was removed and the cells were incubated with 100 μL of LPS 10 μg mL^{-1} for 24 h. After this time 50 μL of supernatant were treated following the protocol provided, while the cells were washed with DPBS and cell viability was evaluated as described for cell viability test.

2.21. Scanning electron microscopy (SEM) analyses

To evaluate the morphology and size of microparticles, small amount of the powder was mounted on a specimen stub with double-sided carbon tape and was coated with gold using a sputter coater; the sample was observed by using a PRO X PHENOM Desktop SEM (Thermo Fisher Scientific, Milan, Italy) and using the ImageJ program to evaluate the size distribution.

2.22. Surface analysis and porosity

The specific surface area and the pore size distribution of the sample were determined using BET equipment from Quantachrome instruments Autosorb iQ and ASiQwin. A weighted sample amount was degassed for 24 h at 40 °C, followed by analysis at -196 °C with N2 as the adsorbate gas.

The nitrogen isotherm was fitted with the Brunauer–Emmett–Teller (BET) model to evaluate the surface area. The pore size distribution and the cumulative pore volume were calculated by the Barrett–Joyner–Halenda (BJH) method.

3. Result and discussion

3.1. Synthesis and characterizations of polymers

The design of a siRNA delivery system must take into account various aspects, such as the ability to bind siRNA and release it into the cytosol of target cells, first passing the cell membrane and then the endosomal-lysosomal membrane.

Synthetic polymeric cations (polycations) represent, in principle, valid candidates in this field, since these can be synthetized with adequate structural and functional properties, conferring specific characteristics necessary for a vector of genetic material (Cavallaro et al., 2017a).

In the present work an α, β-poly (N-2-hydroxyethyl) -D, L-aspartamide (PHEA) derivate has been developed, conjugating 1,2-Bis (3-aminopropylamino) ethane (bAPAE) to the polymeric backbone of PHEA, obtaining the graft copolymer PHEA-g-bAPAE. In this way, a copolymer having protonable amines in the side chain was obtained; the latter confers the ability to complex the genetic material thanks to electrostatic interactions.

Considering that the aim of this work was the delivery of siRNA by inhalation route and therefore locally to the lung, it was decided to functionalize the PHEA-g-bAPAE with Polyethylene glycol, in order to minimize both the phenomenon of aggregation among polyplexes and the interactions with the mucus components of the lungs (Craparo et al., 2016).

Furthermore, considering that the polyplexes must also be able to penetrate the epithelial cells, the surface of polyplexes was functionalized with the TAT peptide, exploiting a *thiol-ene* reaction, which being classified as *click chemistry* is fast, efficient and does not produce by-products.

The synthesis of the PHEA-g-bAPAE copolymer (Scheme 1 step a) involved the activation of the free PHEA hydroxyl groups with bis-nitrophenyl carbonate (BNPC), choosing a stoichiometry of the reagents in order to obtain a ratio between the moles of BNPC and moles of repetitive units of PHEA equal to 0.6.

In the second step of the reaction, a large excess of bAPAE was used, in order to avoid the cross-linking that could occur due to multiple nucleophilic attacks of the side chains since the used oligoamine has two primary amino groups (-NH_2). Under these experimental conditions, a degree of derivatization in bAPAE (DD_{bAPAE}) of the PHEA-g-bAPAE copolymer of about 35% by moles was obtained. The latter was calculated by ^{1}H NMR analysis (Fig. S1) using the ratio between the integral of the signals corresponding to 4H of bAPAE (a δ 1.70 and 2.20 ppm), and the integral of the signal corresponding to 2H of PHEA repeating unit (at δ 2.73 ppm); this was also confirmed by the TNBS colorimetric assay, which provides a DD% value superimposable to that obtained by the ^{1}H NMR analysis (Di Gioia et al., 2015).

The successful conjugation of 1,2-Bis (3-aminopropylamino) ethane (bAPAE) was also demonstrated by the shift of the signal at about δ 4.1, attributed to the side chain CH_2 of the functionalized PHEA repeating unit ($NHCH_2CH_2OCO$—) near the OCONH bond.

In our previous work (Craparo et al., 2020), through potentiometric titrations, it was possible to determine the pKa of the primary amine and of the two secondary amines (which were found to be 10.9, 7.9 and 4.8 respectively) after the conjugation to the polymeric backbone. Thanks to these characteristics, the PHEA-g-bAPAE copolymer has been shown to have an efficient buffering ability in the pH range 7–5, important for endosomal escaping with proton sponge effect (Patel et al., 2019). Furthermore, thanks to its different degree of protonation as a function of pH, when the copolymer is in an acid environment (i.e. endosomal), it is able to destabilize biological membranes, offering an additional mechanism for the endosomal escape process (Miyata et al., 2008; Gao et al., 2015).

In order to insert into PHEA-g-bAPAE structrure PEG chains, able to minimize both aggregation events among polyplexes and the interaction with mucins, NH_2—PEG—COOH derivative was chosen and first functionalized with succinimide ester of 4-Maleimidobutyric acid (MLB-NHS).

This reaction allows to introduce a C═C double bond at the terminal of the PEG aviable for the subsequent thiol-ene reaction.

Furthermore, to avoid the nucleophilic attack of the amino group on the double bond of the maleimide, the pH of the reaction is kept around 7 using DPBS as the reaction solvent.

The successful conjugation was demonstrated by ^{1}H NMR analysis (Fig. S2); in particular, by comparing the integral of the peaks relative to the butyric moiety of the MLB (at 1.87 and 2.27 ppm), corresponding to 2H, with the integral of the peak relative to the repetitive unit of the PEG (at δ 3.72 ppm), corresponding to 176H, it was confirmed that the PEG was functionalized with maleimide moiety, obtaining MLB-PEG-COOH derivative.

The conjugation of the MLB-PEG-COOH to the PHEA-g-bAPAE copolymer (Scheme 1, step c) first involved the activation of the carboxylic group of the PEG-MLB through the use of EDC and NHS, maintaining the pH of the reaction mixture around 6, and subsequently the nucleophilic attack of primary amino groups of the PHEA-g-bAPAE copolymer to the succinimide ester of the NHS-PEG-MLB, keeping the pH of the reaction mixture around 7.

The successful conjugation was demonstrated by ^{1}H NMR analysis (Fig. 1); in particular, the degree of derivatization in PEG ($DD_{\%PEG}$),

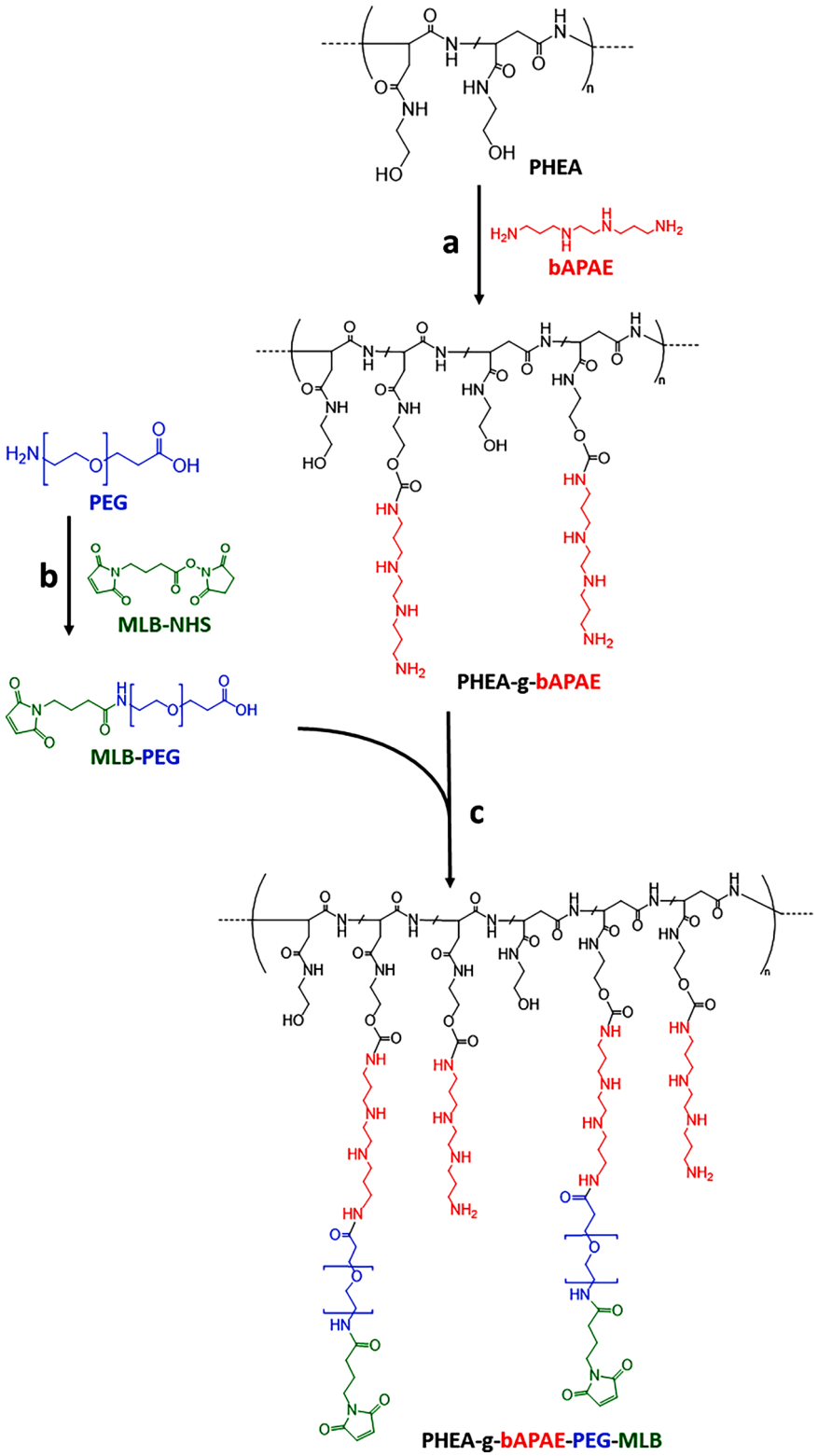

Scheme 1. Synthesis scheme of PHEA-g-bAPAE (a), PEG-MLB (b) and PHEA-g-bAPAE-PEG-MLB copolymer (c). Reagents and experimental conditions: (a) a-DMF, BNPC, 4 h at 40 °C, 20 h at 25 °C; (b) DPBS overnight at 25 °C; (c) MES pH 6, EDC, NHS, 4 h a 25 °C, overnight at 25 °C.

calculated as the ratio between the integral of the signals corresponding to the protons of the repeating unit of PEG (at δ 3.60 ppm), with the integral of the protons corresponding to 2H of the PHEA repeating unit (at δ 2.7 ppm), was founded equal to 4.7 % mol/mol.

All polymers were analyzed by SEC (Table 1). The $\overline{M}_w$ of PHEA-g-bAPAE copolymers undergoes a strong reduction when compared with the $\overline{M}_w$ of PHEA, due to the experimental condition to achieve a high degree of functionalizations (Craparo et al., 2020), as the use of a high amount bAPAE (needed to avoid crosslinking) could break some amide bound in the main chain and thus leading to a shorter polymeric chains.

For PHEA-bAPAE-PEG-MLB graft copolymer an increase in Mw is observed which is compatible with the obtained PEG functionalization.

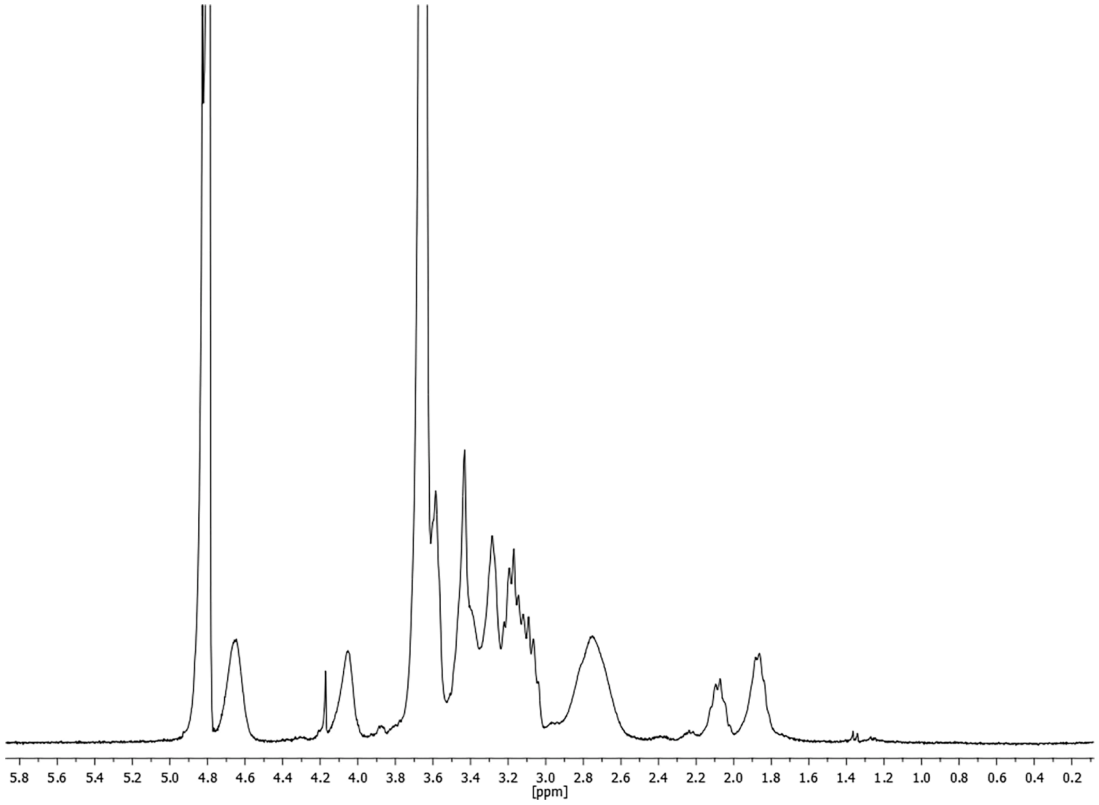

Fig. 1. ^{1}H NMR spectrum in D_2O of PHEA-bAPAE-PEG-MLB.

Table 1
Weight-average molecular weight ($\overline{M}_w$), polydispersity index ($\overline{M}_w$ /$\overline{M}_n$), and chemical composition of obtained copolymers.

Copolymers	Molecular weight		Degree of derivatization (DD%)	
	$\overline{M}_w$ (g/mol)	$\overline{M}_w/\overline{M}_n$	DD_{PEG}	DD_{bAPAE}
PHEA	67,500	1.24	—	—
PHEA-g-bAPAE	20,921	1.41	—	35
PHEA-g-bAPAE-g-PEG-MLB	35,100	1.51	4.7	35

3.2. Introduction of thiol group in TAT peptide

To exploit a thiol-ene reaction, to functionalize the polyplexes on the surface with the TAT peptide, a thiol group was introduced into TAT peptide structure.

The introduction of the thiol group was carried out by exploiting the reactivity of the amino groups present in the peptide towards the succinimide ester of 3- (2-pyridyldithium) propionic acid (SPDP).

Functionalization was confirmed by ^{1}H NMR analysis (Fig. S3). Comparing the peaks corresponding to 4H at the aromatic ring of 3- (2-pyridildithio) propionic acid (4H) (δ 8.3, 7.7 and 7.2 ppm) with the peaks corresponding to 4H of the p-hydroxy benzyl moiety of tyrosine (δ 7.1 and 6.8 ppm) it is possible to confirm the complete functionalization of the peptide.

The product obtained was also analyzed by FT-IR spectroscopy; comparing the IR spectrum of the TAT-SPDP conjugate with that of the unmodified TAT peptide (Fig. 2), a reduction of the characteristic NH bending band at1650 cm^{-1} is observed, indicating a reduction of free primary amino groups present in the peptide. In addition, a new band is observed at 529 cm^{-1}, attributable to the disulfide bridge (Masnabadi et al., 2017) of the SPDP, not present in the original structure of TAT peptide.

In addition, an HPLC analysis was conducted on the obtained derivative which showed a longer retention time (13.87 min) than the unmodified peptide (6.77 min).

The deprotection of the thiol group occurred due to the cleavage of the disulfide bond by the reducing agent dithiothreitol (DTT).

3.3. Complexation study

To evaluate the complexation efficiency of the synthesized copolymer, an agarose gel electrophoresis was performed. In this regard, equal volumes of two dispersions were mixed, one containing siRNA at a fixed concentration and the other containing an increasing concentration of the PHEA-g-bAPAE-PEG-MLB copolymer, in order to obtain different polymer / siRNA weight ratios (R) between 1 and 5.

As it can be seen in Fig. 3, the PHEA-g-bAPAE-PEG-MLB copolymer was able to complex strongly the siRNA strands starting from an R equal to 3 (corresponding to an N / P ratio of 3), a ratio quite low if compared with other synthetic copolymers proposed as non-viral vectors for siRNA delivery (Cavallaro et al., 2017a); this result indicates that the synthesized polymer has an excellent complexing ability of the genetic material, which will allow the use of small quantities of vector for the delivery of the siRNA.

Subsequently, the possibility to functionalize these polyplexes on the surface with the TAT peptide was explored by using the thiol-ene type reaction.

The functionalization efficiency was evaluated by the reaction of a known excess of the peptide (60.5 nmol) with a known amount of polyplexes that contain an amount of maleimide able to bind 50 % of the added peptide (30.25 nmol).

Considering that the reaction between the unsaturation of maleimide and the thiol group reduces the content of thiol groups, the remaining amount of thiol group was determined by Ellman's assay.

As shown in Fig. S4, the absorbance at 410 nm is reduced to about 60 % of the initial value after 2 h of incubation of the peptide with the polyplexes, indicating that almost 40 % of the TAT peptide has been

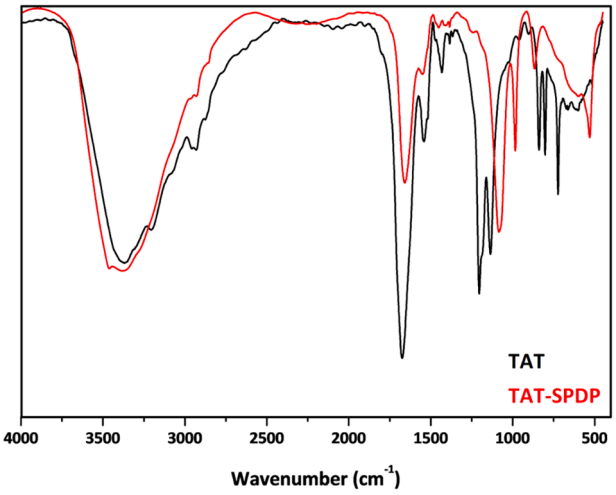

Fig. 2. FT-IR spectrum of TAT-SPDP conjugate (red) and $TAT_{(47-57)}$ peptide (black). (For interpretation of the references to color in this figure legend, the reader is referred to the web version of this article.)

conjugated to the polyplex. Considering that the maximum conjugable amount was 50 % (due to the experimental conditions used), it can be considered that the functionalization reaction proceeds efficiently for about 80 %.

3.4. Cell viability

Considering the potential pulmonary administration of polyplexes, the cytocompatibility of the PHEA-g-bAPAE-PEG-MLB copolymer was evaluated by MTS assay on 16HBE cells, after 24 and 48 h of incubation, expressing the data as % of cell viability respect to control experiment, in which cells are incubated only with OPTI-MEM medium (Fig. 4).

As can be seen, both after 24 and 48 h of incubation, only for the highest tested concentration (0.5 mg mL^{-1}) show viability slightly lower than 80 %, while the other concentrations tested show cell viability higher than 80 %, indicating good cytocompatibility.

Considering that siRNAs exert their inhibitory effect in quantities of the order of picomoles (Cavallaro et al., 2017a), the amount of polymer required for the delivery of a therapeutic quantity of siRNA is very low (<0.001 mg mL^{-1}), a quantity for which the PHEA-g-bAPAE-PEG-MLB copolymer shows excellent cytocompatibility.

The viability assay carried out on cells incubated with polyplexes

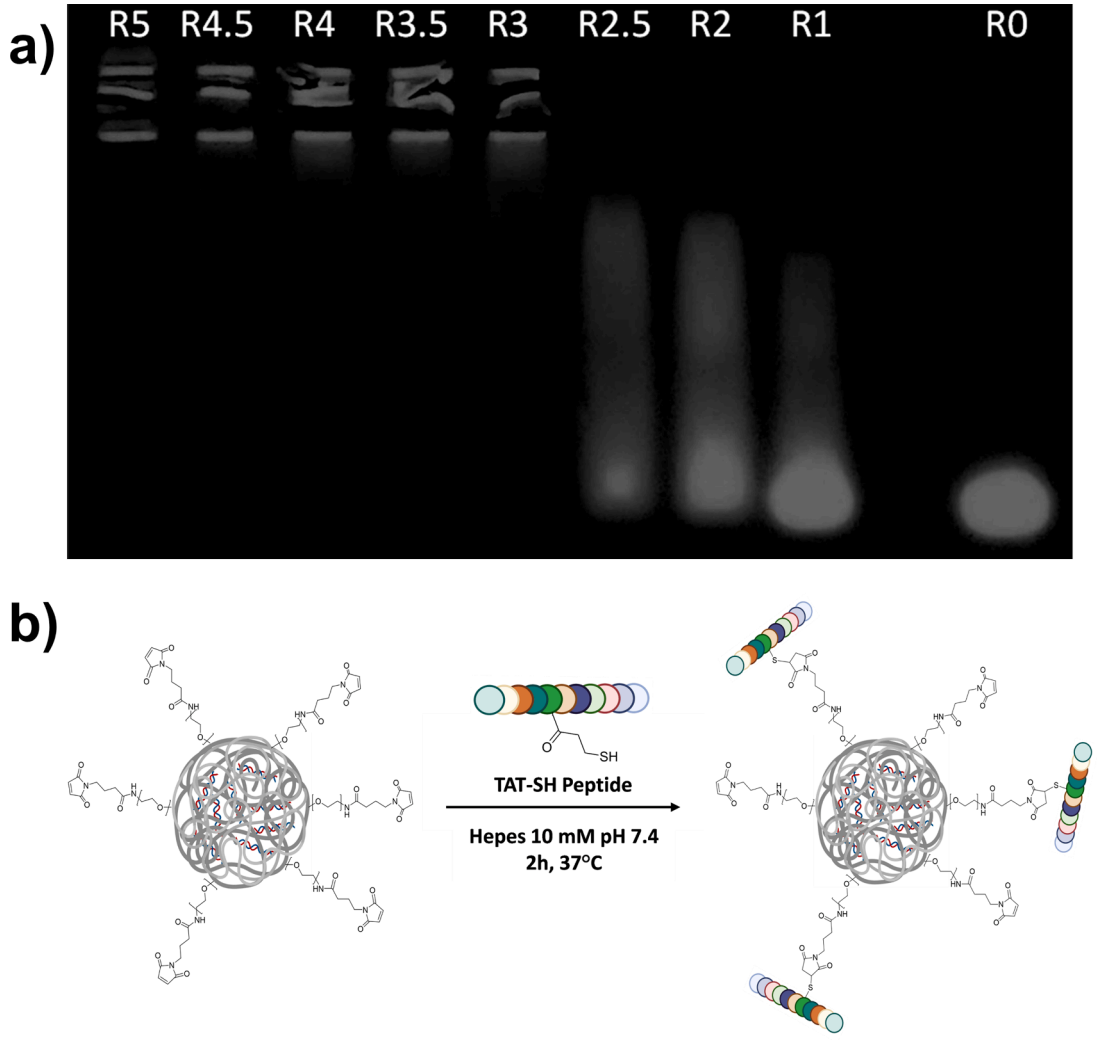

Fig. 3. (a) Agarose gel electrophoresis of the polyplexes obtained in 10 mM HEPES at various weight ratios PHEA-g-bAPAE-PEG-MLB / siRNA (R); (b) Schematic representation of surface functionalization.

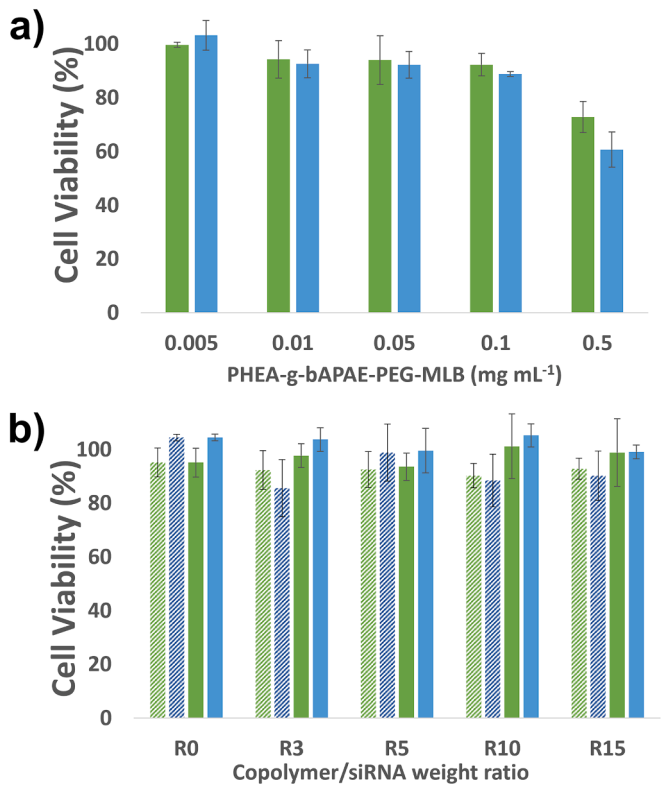

Fig. 4. Cell viability of 16HBE after 24 (green) and 48 (blue) hours of incubation with: (a) PHEA-g-bAPAE-PEG-MLB; (b) PHEA-g-bAPAE-PEG-MLB / siRNA polyplexes functionalized with TAT peptide (full square) or not (dashed square), at different weight ratio (R) (data are reported as means SD, $n = 3$). (For interpretation of the references to color in this figure legend, the reader is referred to the web version of this article.)

(obtained in order to have a final concentration of siRNA equal to 100 nM), both functionalized with TAT peptide and non-functionalized, shows excellent cell viability values for all weight ratios. tested, both after 24 and 48 h of incubation (Fig. 4).

3.5. Stability to polyanionic exchange

Since the polyplexes are designed to be administered by inhalation, it was necessary to evaluate their stability in presence of mucins.

In particular, given the polyanionic nature of the mucin (due to the presence of sialic acid residues), a polyanionic exchange can occur between siRNA and mucin. Therefore, a study was carried out evaluating the electrophoretic mobility of siRNA in polyplexes, obtained with R equal to 5 and 10, functionalized or not with the TAT peptide, in the presence of mucin in the dispersion medium. Before performing electrophoresis, polyplexes were incubated for 5 h in a mucin dispersion having a final concentration of 1 mg mL^{-1}.

As a comparison, the electrophoretic run was performed both on siRNA naked (R0) and polyplexes not incubated with mucin previously.

As can be seen in Fig. 5, only the polyplexes prepared with the highest weight ratio (R = 10) avoid the polyanion exchange between siRNA and mucin, preserving from premature release of siRNA; furthermore, the presence of the TAT peptide, despite being a cationic peptide that could increase the stability of the polyplexes, does not seem to influence this phenomenon.

Therefore, considering that only the polyplexes obtained with a weight ratio equal to 10 (R10) are stable in the presence of mucin, subsequent studies have been carried out exclusively on these polyplexes.

3.6. Dynamic light scattering

The average dimensions and the surface charge of the polyplexes, obtained with *R* equal to 10, were evaluated by dynamic light scattering measurements.

As reported in Table 2, the PHEA-g-bAPAE-PEG-MLB / siRNA polyplexes have sizes slightly larger than 100 nm and a slightly positive surface charge, which however allows to avoid aggregation phenomena.

After functionalization with TAT peptide, a slight increase in the hydrodynamic radius of about 17 nm and an increase in the surface charge of about 10 mV is observed, correlated to the presence of the different guanidine groups present in the peptide.

These dimensions are appropriate to allow diffusion through mucus layer, as it is estimated that airway mucus has pore sizes of about 200 nm (Duncan et al., 2016a). At the same time, however, it should be noted that the diffusion process depends on various factors, so it is necessary to carry out further investigations in this regard.

3.7. Evaluation of interaction with mucins

Considering that the negative charge of the mucin can not only give rise to polyanionic exchange, but also may lead to the formation of aggregates between polyplexes and mucins, a turbidimetric analysis was conducted as a function of the incubation time, considering that the occurrence of *polyplexes-mucin* interactions, involves a reduction in the transmittance of the dispersion. The data, shown in Fig. 5, are expressed as a percentage of transmittance (respect to the transmittance of a mucin dispersion 1 mg mL^{-1}) as a function of the incubation time.

For the polyplexes obtained with PHEA-g-bAPAE-PEG-MLB, the approximately linear reduction of the% of transmittance indicates a tendency to interact with mucin, in particular in the first 200 min; otherwise, for longer incubation times, the inversion of this trend is observed, indicating that the *polyplexes-mucin* interactions are reduced over time.

For polyplexes obtained with PHEA-g-bAPAE-PEG-MLB functionalized on the surface with TAT peptide, the tendency to interact with mucin is more evident in the first incubation times (% transmittance equal to 55); this behavior is related to the higher positive charge due to the presence of the TAT, as suggested by the zeta potential data.

As for non-functionalized polyplexes, a variation of the % of transmittance is observed over time; in particular the % of transmittance is almost static (about 55 %) up to 100 min and subsequently a slow and gradual increase of the same is observed.

The reduction of polyplexes-mucin interactions as a function of time indicates that these interactions are reversible and therefore could, in principle, not hinder the diffusion of polyplexes in the mucus.

To verify if these interactions could reduce the diffusion of polyplexes throw the mucus layer, a mucopenetration test was performed following a protocol reported in the literature (Lock et al., 2018), using inserts for cell plates, equipped with a hydrophilic polypropylene membrane with pores of 0.45 μm, upon which a mucin dispersion has been deposited to have a thickness of about 1.3 mm.

The dispersion containing the PHEA-g-bAPAE-PEG-MLB / siRNA polyplexes functionalized with TAT peptide was deposited on the mucin dispersion and the fluorescence intensity at λ 665 nm in the recipient compartment was measured at scheduled times.

As shown in Fig. 5, the presence of mucins upon the membrane is not able to hinder the passage to the recipient compartment, but only to slow down the diffusion of polyplexes if compared to the simple diffusion (evaluated with the same system, but in the absence of mucin).

In particular, it is observed that the polyplexes functionalized with TAT peptide can cross effectively the barrier represented by the mucin network, reaching the receiving compartment within 5 h in quantities corresponding to about 90 % of the total.

However, it should be noted that commercially available purified mucins do not readily form a viscoelastic gel with rheological properties

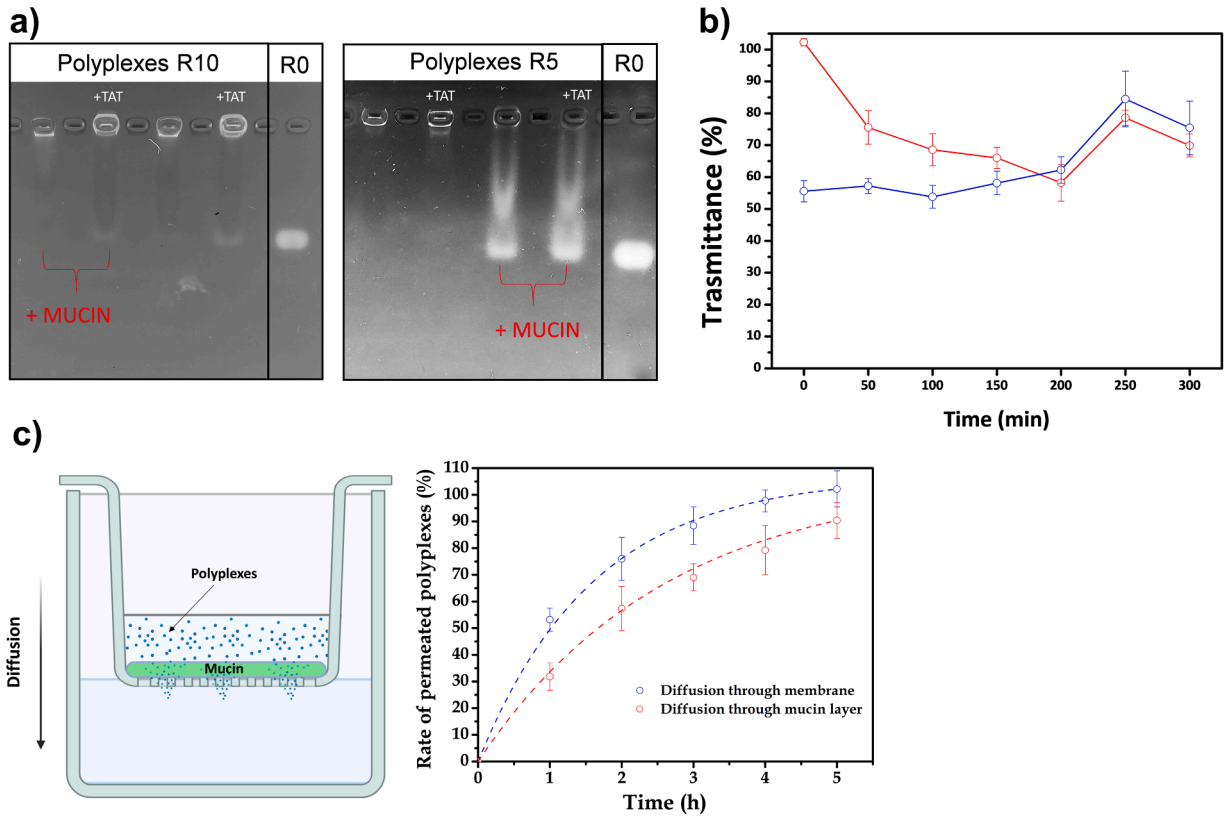

Fig. 5. (a) Evaluation of the electrophoretic mobility of siRNA in the polyplexes obtained with R10 and R5, functionalized and non-functionalized with TAT, after 5 h of incubation with and without mucin; (b) transmittance at 500 nm of dispersions containing mucin in the presence of PHEA-g-bAPAE-PEG-MLB / siRNA (R10) polyplexes, non-functionalized (red line) and functionalized with TAT (blue line) (Data are reported as means SD, $n = 3$); (c) schematic representation of the system used and quantification of polyplexes (%) that reach the recipient compartment in the mucopenetration test, compared with diffusion through hydrophilic polypropylene membrane (Data are reported as means SD, $n = 3$). (For interpretation of the references to color in this figure legend, the reader is referred to the web version of this article.)

Table 2
Z-average, polydispersity index (PDI), Z potential of polyplexes.

Polyplexes	Z-average (nm)	PDI	Z potential (mV)
PHEA-g- bAPAE-PEG-MLB/ siRNA (R10)	107±14	0.366 ± 0.109	+10.9 ± 5.7
PHEA-g- bAPAE-PEG-MLB/ siRNA (R10) + TAT	124 ± 21	0.531 ± 0.043	+21.0 ± 13.8

comparable to native mucus samples at physiological concentrations (Duncan et al., 2016b). For this reason, only the effects that electrostatic interactions have on the passage of the polyplexes through the mucin layer are taken into account in this study.

3.8. Cell uptake studies

To assess the ability of polyplexes to be endocytosed by the cells of the bronchial epithelium, uptake studies were conducted on 16HBE cells.

As can be seen in Fig. 6, after 4 h of incubation the polyplexes functionalized with the TAT peptide begin to be present in the cytoplasm of the cells, as indicated by the weak visible fluorescence; differently, the non-functionalized polyplexes and the siRNA naked are not visible. After 24 h of incubation, an increase in fluorescence is observed, implying that cell internalization in 16-HBE is time dependent. Furthermore, for polyplexes functionalized with the TAT peptide, the fluorescence is higher when compared with that recorded for non-functionalized polyplexes, indicating a greater cellular internalization. At the same time, the fluorescence recorded for non-functionalized polyplexes is in any case higher than that recorded for cells incubated with siRNA naked.

Subsequently, quantitative uptake studies were carried out after 4 and 24 h of incubation, evaluating the fluorescence of the siRNA-Cy5 contained in the cell lysate.

Fig. 6 shows the normalized fluorescence intensity per mg of proteins contained in the same cell lysate.

After 4 h of incubation, the amount of internalized siRNA after incubation with polyplexes functionalized with the TAT peptide is approximately 3 times higher than that internalized after incubation with non-functionalized polyplexes.

After 24 h of incubation, an increase in fluorescence intensity is recorded in both cases, confirming the time-dependent behavior observed by fluorescence microscopy (Fig. 6) and confirming that polyplexes functionalized with TAT peptide were internalized more efficiently than non-functionalized polyplexes.

3.9. Gene silencing assay

Once demonstrated that these polyplexes are stable and could be effectively administered by inhalation, as they can penetrate through the mucin layer and be internalized by the cells of the bronchial epithelium, the gene silencing capacity of obtained polyplexes was evaluated by *in vitro* ELISA test upon 16HBE cells.

Cells were treated with: (a) naked siRNA and (b) polyplexes and (c) polyplexes decorated with TAT, both obtained with R equal to 10, and then exposed to an inflammatory agent, such as LPS. Relative IL-8 production (percentage) was expressed as (Abs treated cells/Abs positive control cells) × 100. Obtained values are reported in Fig. 7.

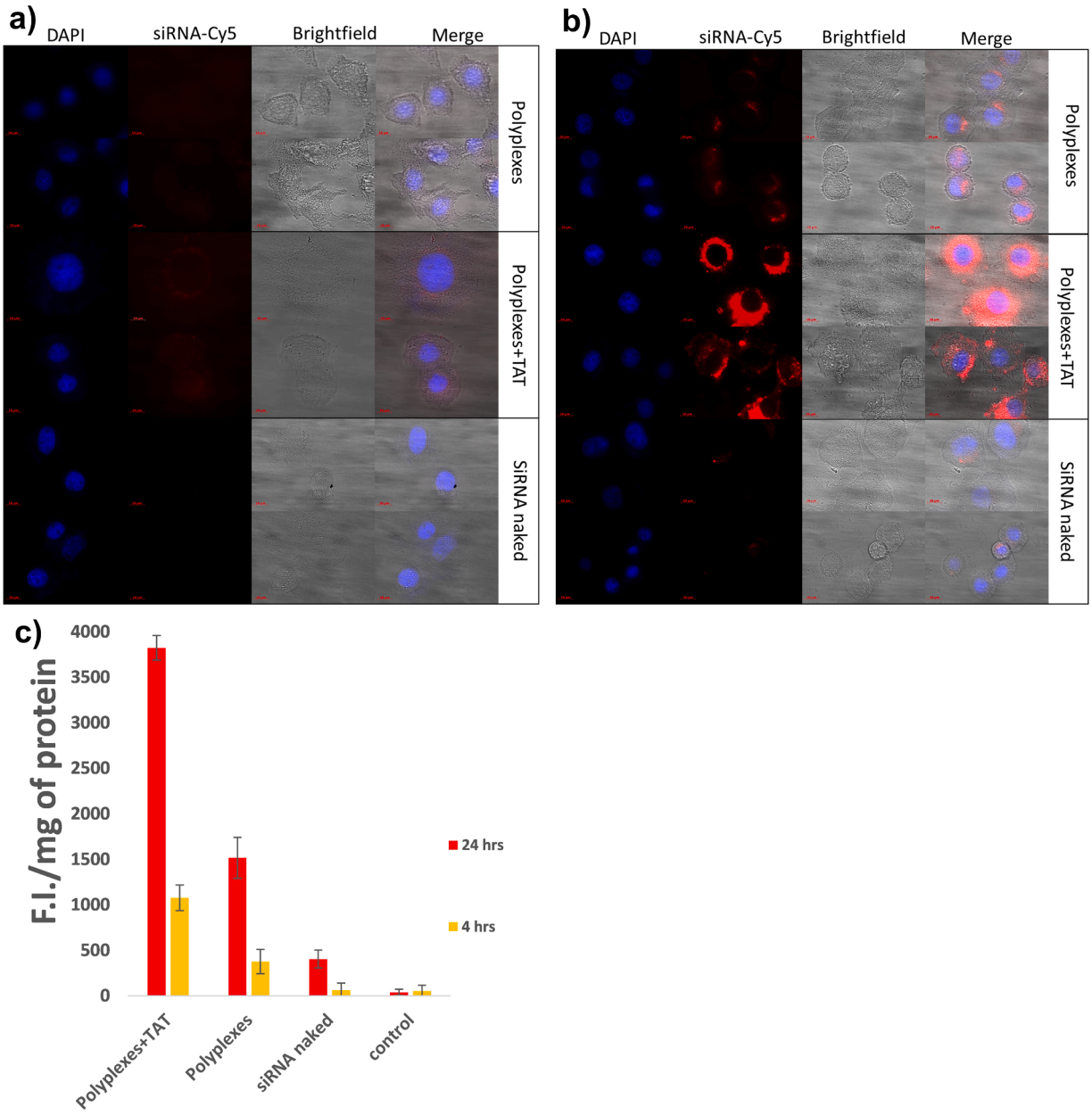

Fig. 6. Qualitative uptake of PHEA-g-bAPAE-PEG-MLB / siRNA-Cy5 polyplexes on human bronchial epithelium cell culture (16HBE) after 4 h (a) and 24 h (b) 100X; (c) quantitative uptake of PHEA-g-bAPAE-PEG-MLB / siRNA-Cy5 polyplexes on human bronchial epithelial cell culture (16HBE) after 4 h and 24 h (Data are reported as means SD, $n = 3$).

Obtained results show that cells incubated with naked siRNA produce an IL-8 amount non significantly different from that obtained with control cells. Differently, when cells are incubated in the presence of polyplexes, there is a reduction of about 30 % in the expression of IL-8.

More promising results have been obtained with the polyplexes decorated with TAT peptide, since the silencing efficiency is almost doubled (-60 % of IL-8 expressed). This higher silencing efficiency is correlated to the higher cellular internalization efficiency when polyplexes are functionalized on the surface with TAT peptide, as demonstrated in previous uptake studies.

Furthermore, the viability of the treated cells was found to be close to 100 %, thus demonstrating that the reduction in IL-8 production is not caused by cell death.

In parallel, the same experiment was conducted using a siRNA sequence inactive on the cell line used, not recording any reduction in the amount of IL-8 produced and therefore correlating the pharmacological activity to the specific siRNA sequence.

3.10. *Microparticles preparation and characterization*

Powders of nanosized particles are not suitable for direct inhalation, since dimensions are not suitable for bronchial deposition (d'Angelo et al., 2014). To overcome this problem, one of the possible strategies is the Nano into Micro strategy (NiM), where the nanosystems are encapsulated in water-soluble microparticles, which dissolve once in contact with lung fluids, releasing nanosystems (Drago et al., 2021).

In particular, here, spray freeze drying was chosen as an easy technique which allow to produce highly porous dry powder particles from an aqueous sample solution (Okuda et al., 2018), allowing to work at low temperatures, thus preserving the integrity of siRNAs (Liang et al., 2018).

As matrix material to produce inhalable microparticles, mannitol

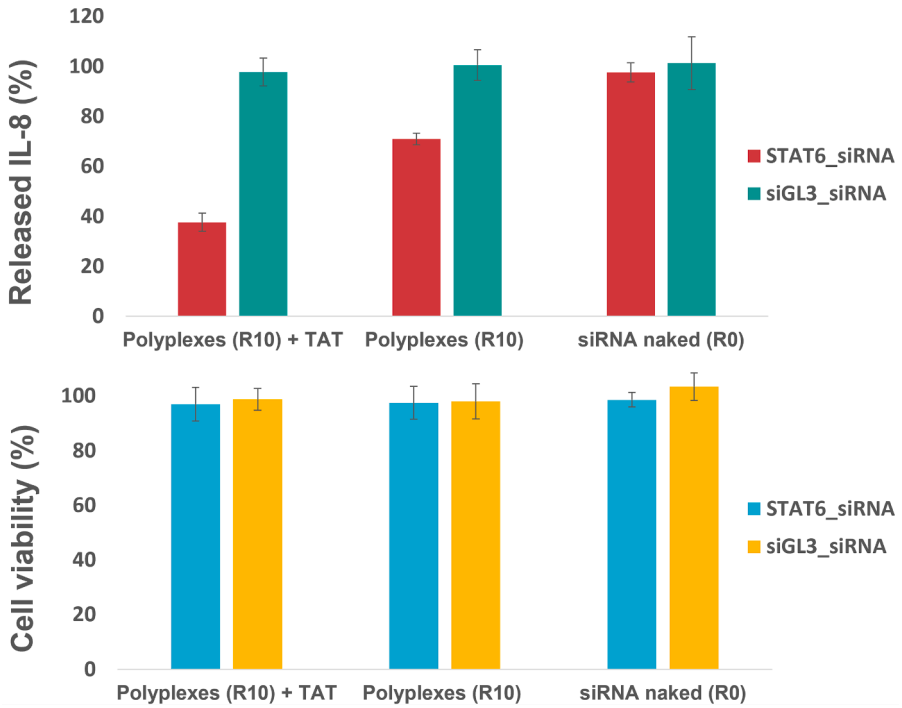

Fig. 7. IL-8 (%) released by 16HBE cells after incubation with polyplexes or with naked siRNA for 48 h, compared to a positive control, and cell viability (Data are reported as means SD, $n = 3$).

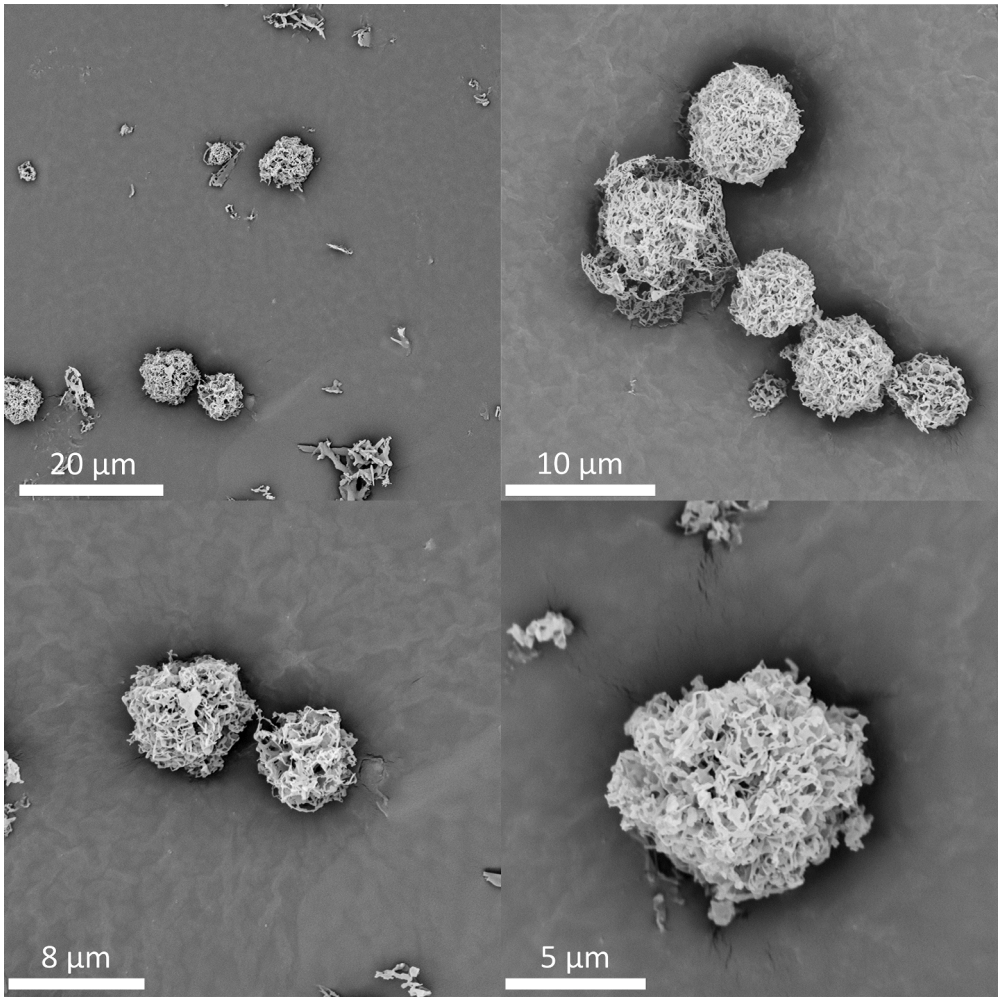

Fig. 8. SEM micrographs of the mannitol porous microparticles containing polyplexes obtained by spray freeze drying.

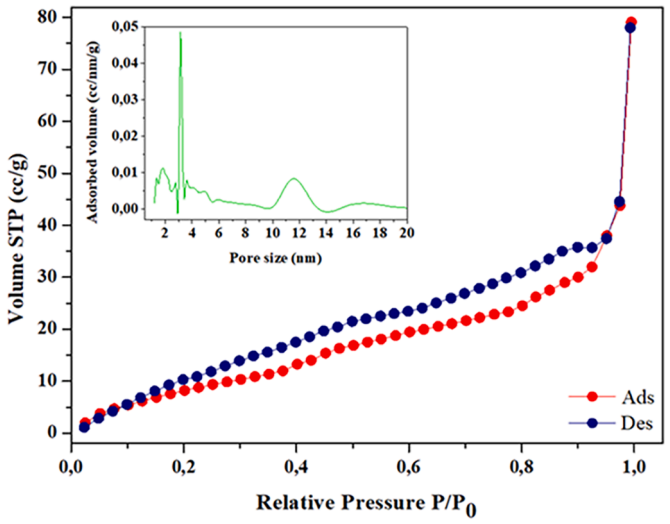

Fig. 9. BET nitrogen adsorption-desorption linear isotherm of the sample. Inset graph represents the pore size distribution calculated using the BJH method according to the desorption isotherm.

was chosen because of its ability to induce the influx of water from the epithelial cell layer to the mucus (thanks to its osmotic nature), with a consequent change in the viscoelastic properties of the mucus (Craparo et al., 2016; Porsio et al., 2017; Daviskas et al., 2010).

First, we quantified the siRNA content into the microparticles and compared it with that of fresh polyplexes preparation, using an ethidium bromide (EtBr) exclusion assay as described in the experimental part. The data obtained showed that no siRNA losses, due to degradation, occur.

Then, the actual ability of this system to induce gene silencing, even after spray freeze-drying, was then assessed using *in vitro* assays that quantified IL-8 released by treated cells after exposure to LPS. In particular, polyplexes were found to retain excellent silencing capacity, reducing IL-8 release by approximately 50 % (Fig. S5).

The spray freeze-drying technique is therefore an excellent drying method for nucleic acid-based drug delivery systems, as it avoids nucleic acid degradation which leads to a reduction in the pharmacological effect.

In consideration that the properties of inhaled powders critically influenced the aerosolization efficiency of DPIs and consequently the deposition site in the respiratory tract, the morphology, the specific surface area and the porosity were further investigated by Scanning Electronic Microscopy and by gas physisorption.

The SEM micrographs of the obtained powder (Fig. 8) show that the particles obtained with this technique have an irregular but almost spherical shape, with an average physical diameter of about 7 μm, and are characterized by high porosity.

Therefore, in order to investigate the surface characteristics of the particles, the Brunauer–Emmett–Teller (BET) method is applied to calculate the specific surface area, while the Barrett, Joyner and Halenda (BJH) model was used to calculate the pore size distribution.

Fig. 9 shows the nitrogen adsorption-desorption isotherm and the corresponding Barret–Joyner–Halenda (BJH) pore size distribution curve of the obtained sample.

According to IUPAC classification, the sample exhibits a type IVa isotherm with a H3-type hysteresis loop characteristic of mesoporous materials and attributable to particles with lamella-shaped pores (Thommes et al., 2015; Sun et al., 2017). This fits with the obtained pore size distribution (Fig. 9 inset) which shows that the pores are mostly mesoporous, falling into the range of 2–50 nm.

The external surface area, calculated by the BET equation from nitrogen adsorption data, was 47.269 m^2g^{-1} (multi-point BET). In addition, the total pore volume was 0.135 ($cm^3\ g^{-1}$).

Considering that particles of the same size (7 μm), perfectly spherical, consisting of pure mannitol ($d_{mannitol}$= 1.49 g cm^{-3}), have a specific surface area of about 0.57 $m^2\ g^{-1}$, our particles have a specific surface area about 80 times higher, having a high porosity that could allow powder aerosolization.

4. Conclusions

In this work, polyplexes able to release siRNA in the bronchial epithelium as a possible treatment of asthma were designed using a cationic copolymer derived from PHEA.

To obtain a protonable copolymer, PHEA was first conjugated with the oligoamine bAPAE and subsequently with an appropriate amount of PEG, which, as widely known, modulating the hydrophilicity and shielding the charge of the nanocomplexes, confer the ability to penetrate through the mucus layer.

Furthermore, considering that these polyplexes must be able to cross not only the mucus barrier, but also the barrier represented by the bronchial epithelium, polyplexes were functionalize on the surface with the TAT peptide, exploiting a thiol-ene reaction, by introducing thiol group in TAT structure and introducing a double bond to the PEG chain.

The introduction of a double bond at the PEG terminal was obtained using a derivative of maleimide, obtaining the MLB-PEG-COOH derivative which was subsequently conjugated to the PHEA-g-bAPAE copolymer, using EDC and NHS as condensating agents. The introduction of the thiol group into the peptide structure was achieved by using the succinimide ester of 3- (2-pyridyldithium) propionic acid (SPDP).

Therefore, nanometric (≈ 124 nm) polyplexes decorated on the surface with the TAT peptide have been obtained; these results to be cytocompatible and able to retain the siRNA with a suitable complexation R during the diffusion process through the mucus.

Despite polyplexes establish weak bonds with the mucin chains, these can diffuse efficiently through the mucin layer and therefore they are potentially able to reach the bronchial epithelium.

Furthermore, through cellular uptake studies, it was possible to observe how the obtained polyplexes penetrate effectively in the cytoplasm of bronchial epithelial cells, where they can reduce IL-8 gene expression of 30 % and 60 %, respectively for nude polyplexes and TAT decorated polyplexes, after LPS exposure.

In the end, polyplexes were encapsulated in water soluble mannitol-based microparticles, by spray freeze drying, obtaining highly mesoporous structures of about 7 μm and a specific surface area equal to 47.269 m^2g^{-1}, characteristics that make them potentially administrable by inhalation route.

^{1}H NMR spectra of PHEA-bAPAE copolymer, MLB-PEG-COOH derivative and TAT-SPDP conjugate. Quantitative determination of surface functionalization with TAT peptide.

CRediT authorship contribution statement

Salvatore Emanuele Drago: Conceptualization, Methodology, Formal analysis, Investigation, Data curation, Writing – review & editing. **Marta Cabibbo:** Methodology, Formal analysis, Investigation, Data curation, Writing – review & editing. **Emanuela Fabiola Craparo:** Conceptualization, Supervision, Data curation, Writing – review & editing. **Gennara Cavallaro:** Conceptualization, Supervision, Data curation, Writing – review & editing.

Data availability

No data was used for the research described in the article.

Funding Sources

This work was supported by University of Palermo.

Acknowledgment

The authors thank the Advanced Technologies Network Center (ATeNCenter) of the University of Palermo-Laboratory of Preparation and Analysis of Biomaterials for analytical instruments and Mr. Francesco Paolo Bonomo for technical support.

Supplementary materials

Supplementary material associated with this article can be found, in the online version, at doi:10.1016/j.ejps.2023.106580.

References

Ali, A.K., Hartzema, A.G., 2012. Assessing the association between omalizumab and arteriothrombotic events through spontaneous adverse event reporting. J. Asthma Allergy 5, 1–9. https://doi.org/10.2147/JAA.S29811.

Ballarín-González, B., Howard, K.A., 2012. Polycation-based nanoparticle delivery of RNAi therapeutics: adverse effects and solutions. Adv. Drug Deliv. Rev. 64, 1717–1729. https://doi.org/10.1016/J.ADDR.2012.07.004.

Beck, I.M.E., Vanden Berghe, W., Vermeulen, L., Yamamoto, K.R., Haegeman, G., De Bosscher, K., 2009. Crosstalk in inflammation: the interplay of glucocorticoid receptor-based mechanisms and kinases and phosphatases. Endocr. Rev. 30, 830–882. https://doi.org/10.1210/er.2009-0013.

Cavallaro, G., Sardo, C., Craparo, E.F., Porsio, B., Giammona, G., 2017a. Polymeric nanoparticles for siRNA delivery: production and applications. Int. J. Pharm. 525, 313–333. https://doi.org/10.1016/j.ijpharm.2017.04.008.

Cavallaro, G., Farra, R., Craparo, E.F., Sardo, C., Porsio, B., Giammona, G., Perrone, F., Grassi, M., Pozzato, G., Grassi, G., Dapas, B., 2017b. Galactosylated polyaspartamide copolymers for siRNA targeted delivery to hepatocellular carcinoma cells. Int. J. Pharm. 525, 397–406. https://doi.org/10.1016/j.ijpharm.2017.01.034.

Charrad, R., Kaabachi, W., Rafrafi, A., Berraies, A., Hamzaoui, K., Hamzaoui, A., 2017. IL-8 gene variants and expression in childhood asthma. Lung 195, 749–757. https://doi.org/10.1007/s00408-017-0058-6.

Chung, K.F., Wenzel, S.E., Brozek, J.L., Bush, A., Castro, M., Sterk, P.J., Adcock, I.M., Bateman, E.D., Bel, E.H., Bleecker, E.R., Boulet, L.P., Brightling, C., Chanez, P., Dahlen, S.E., Djukanovic, R., Frey, U., Gaga, M., Gibson, P., Hamid, Q., Jajour, N.N., Mauad, T., Sorkness, R.L., Teague, W.G., 2014. International ERS/ATS guidelines on definition, evaluation and treatment of severe asthma. Eur. Respir. J. 43, 343–373. https://doi.org/10.1183/09031936.00202013.

Cooper, B.M., Putnam, D., 2016. Polymers for siRNA delivery: a critical assessment of current technology prospects for clinical application. ACS Biomater. Sci. Eng. https://doi.org/10.1021/acsbiomaterials.6b00363 acsbiomaterials.6b00363.

Craparo, E.F., Porsio, B., Sardo, C., Giammona, G., Cavallaro, G., 2016. Pegylated polyaspartamide−polylactide-based nanoparticles penetrating cystic fibrosis artificial mucus. Biomacromolecules 17, 767–777. https://doi.org/10.1021/acs.biomac.5b01480.

Craparo, E.F., Drago, S.E., Mauro, N., Giammona, G., Cavallaro, G., 2020. Design of new polyaspartamide copolymers for siRNA delivery in antiasthmatic therapy. Pharmaceutics 12, 89. https://doi.org/10.3390/pharmaceutics12020089.

d'Angelo, I., Conte, C., La Rotonda, M.I., Miro, A., Quaglia, F., Ungaro, F., 2014. Improving the efficacy of inhaled drugs in cystic fibrosis: challenges and emerging drug delivery strategies. Adv. Drug Deliv. Rev. 75, 92–111. https://doi.org/10.1016/j.addr.2014.05.008.

d'Ancona, G., Kavanagh, J., Roxas, C., Green, L., Fernandes, M., Thomson, L., Dhariwal, J., Nanzer, A.M., Jackson, D..J, Kent, B.D., 2020. Adherence to corticosteroids and clinical outcomes in mepolizumab therapy for severe asthma. Eur. Respir. J. 55, 1902259. https://doi.org/10.1183/13993003.02259-2019.

Daka, A., Peer, D., 2012. RNAi-based nanomedicines for targeted personalized therapy. Adv. Drug Deliv. Rev. 64, 1508–1521. https://doi.org/10.1016/J.ADDR.2012.08.014.

Darcan-Nicolaisen, Y., Meinicke, H., Fels, G., Hegend, O., Haberland, A., Kühl, A., Loddenkemper, C., Witzenrath, M., Kube, S., Henke, W., Hamelmann, E., 2009. Small interfering RNA against transcription factor STAT6 inhibits allergic airway inflammation and hyperreactivity in mice. J. Immunol. 182, 7501–7508. https://doi.org/10.4049/jimmunol.0713433.

Dave, R.S., Goostrey, T.C., Ziolkowska, M., Czerny-Holownia, S., Hoare, T., Sheardown, H., 2021. Ocular drug delivery to the anterior segment using nanocarriers: a mucoadhesive/mucopenetrative perspective. J. Control Release 336, 71–88. https://doi.org/10.1016/J.JCONREL.2021.06.011.

David, S., Pitard, B., Benoît, J.P., Passirani, C., 2010. Non-viral nanosystems for systemic siRNA delivery. Pharmacol. Res. 62, 100–114. https://doi.org/10.1016/j.phrs.2009.11.013.

Daviskas, E., Anderson, S.D., Young, I.H., 2010. Effect of mannitol and repetitive coughing on the sputum properties in bronchiectasis. Respir. Med. 104, 371–377. https://doi.org/10.1016/J.RMED.2009.10.021.

Di Gioia, S., Sardo, C., Belgiovine, G., Triolo, D., D'Apolito, M., Castellani, S., Carbone, A., Giardino, I., Giammona, G., Cavallaro, G., Conese, M., 2015. Cationic polyaspartamide-based nanocomplexes mediate siRNA entry and down-regulation of the pro-inflammatory mediator high mobility group box 1 in airway epithelial cells. Int. J. Pharm. 491, 359–366. https://doi.org/10.1016/j.ijpharm.2015.06.017.

Drago, S.E., Craparo, E.F., Luxenhofer, R., Cavallaro, G., 2021. Development of polymer-based nanoparticles for zileuton delivery to the lung: PMeOx and PMeOzi surface chemistry reduces interactions with mucins. Nanomed. Nanotechnol. Biol. Med. 37, 102451 https://doi.org/10.1016/J.NANO.2021.102451.

Duncan, G.A., Jung, J., Hanes, J., Suk, J.S., 2016b. The mucus barrier to inhaled gene therapy. Mol. Ther. 24, 2043–2053. https://doi.org/10.1038/mt.2016.182.

G.A. Duncan, J. Jung, J. Hanes, J.S. Suk, The mucus barrier to inhaled gene therapy, (2016a). doi:10.1038/mt.2016.182.

Gao, H., Takemoto, H., Chen, Q., Naito, M., Uchida, H., Liu, X., Miyata, K., Kataoka, K., 2015. Regulated protonation of polyaspartamide derivatives bearing repeated aminoethylene side chains for efficient intracellular siRNA delivery with minimal cytotoxicity. Chem. Commun (Camb) 51, 3158–3161. https://doi.org/10.1039/c4cc09859e.

García-Díaz, M., Birch, D., Wan, F., Nielsen, H.M., 2018. The role of mucus as an invisible cloak to transepithelial drug delivery by nanoparticles. Adv. Drug Deliv. Rev. 124, 107–124. https://doi.org/10.1016/j.addr.2017.11.002.

Georas, S.N., Donohue, P., Connolly, M., Wechsler, M.E., 2021. JAK inhibitors for asthma. J. Allergy Clin. Immunol. 148, 953–963. https://doi.org/10.1016/J.JACI.2021.08.013.

Giammona, G., Carlisi, B., Palazzo, S., 1987. Reaction of α,β-poly(N-hydroxyethyl)-DL-aspartamide with derivatives of carboxylic acids. J. Polym. Sci. Part A Polym. Chem. 25, 2813–2818. https://doi.org/10.1002/pola.1987.080251016.

Global Initiative for Asthma - GINA, (n.d.) 2023.

Gorabi, A.M., Kiaie, N., Aslani, S., Jamialahmadi, T., Johnston, T.P., Sahebkar, A., 2020. Prospects for the potential of RNA interference in the treatment of autoimmune diseases: small interfering RNAs in the spotlight. J. Autoimmun. 114, 102529 https://doi.org/10.1016/j.jaut.2020.102529.

Gour, N., Wills-Karp, M., 2015. IL-4 and IL-13 signaling in allergic airway disease. Cytokine 75, 68–78. https://doi.org/10.1016/J.CYTO.2015.05.014.

Grießinger, J., Dünnhaupt, S., Cattoz, B., Griffiths, P., Oh, S., Gómez, S.B.I., Wilcox, M., Pearson, J., Gumbleton, M., Abdulkarim, M., Pereira De Sousa, I., Bernkop-Schnürch, A., 2015. Methods to determine the interactions of micro- and nanoparticles with mucus. Eur. J. Pharm. Biopharm. 96, 464–476. https://doi.org/10.1016/j.ejpb.2015.01.005.

He, Y., Liang, Y., Han, R., Lu, W.L., Mak, J.C.W., Zheng, Y., 2019. Rational particle design to overcome pulmonary barriers for obstructive lung diseases therapy. J. Control Release 314, 48–61. https://doi.org/10.1016/j.jconrel.2019.10.035.

Healey, G.D., Evans, N., Hopkin, J.M., Davies, G., Walker, W., 2013. Evaluation of nasal epithelium sampling as a tool in the preclinical development of siRNA-based therapeutics for asthma. J. Cell. Mol. Med. 17, 356–364. https://doi.org/10.1111/jcmm.12014.

Heffler, E., Madeira, L.N.G., Ferrando, M., Puggioni, F., Racca, F., Malvezzi, L., Passalacqua, G., Canonica, G.W., 2018. Inhaled corticosteroids safety and adverse effects in patients with asthma. J. Allergy Clin. Immunol. Pract. 6, 776–781. https://doi.org/10.1016/J.JAIP.2018.01.025.

Itaka, K., Yamauchi, K., Harada, A., Nakamura, K., Kawaguchi, H., Kataoka, K., 2003. Polyion complex micelles from plasmid DNA and poly(ethylene glycol)-poly(L-lysine) block copolymer as serum-tolerable polyplex system: physicochemical properties of micelles relevant to gene transfection efficiency. Biomaterials 24, 4495–4506. https://doi.org/10.1016/S0142-9612(03)00347-8.

Jackson, D.J., Bacharier, L.B., 2021. Inhaled corticosteroids for the prevention of asthma exacerbations. Ann. Allergy Asthma Immunol. 127, 524–529. https://doi.org/10.1016/J.ANAI.2021.08.014.

Kay, A.B., 2005. The role of eosinophils in the pathogenesis of asthma. Trends Mol. Med. 11, 148–152. https://doi.org/10.1016/j.molmed.2005.02.002.

Kay, A.B., 2006. The role of T lymphocytes in asthma. Chem. Immunol. Allergy 91, 59–75. https://doi.org/10.1159/000090230.

Koli, U., Krishnan, R.A., Pofali, P., Jain, R., Dandekar, P., 2014. SiRNA-based therapies for pulmonary diseases. J. Biomed. Nanotechnol. 10, 1953–1997. https://doi.org/10.1166/jbn.2014.1928.

Kraft, M., Martin, R.J., Wilson, S., Djukanovic, R., Holgate, S.T., 1999. Lymphocyte and eosinophil influx into alveolar tissue m nocturnal asthma. Am. J. Respir. Crit. Care Med. 159, 228–234. https://doi.org/10.1164/ajrccm.159.1.9804033.

Kubczak, M., Michlewska, S., Bryszewska, M., Aigner, A., Ionov, M., 2021. Nanoparticles for local delivery of siRNA in lung therapy. Adv. Drug Deliv. Rev. 179, 114038 https://doi.org/10.1016/J.ADDR.2021.114038.

Li, N., Song, Y., Zhao, W., Han, T., Lin, S., Ramirez, O., Liang, L., 2016. Small interfering RNA targeting NF-κB attenuates lipopolysaccharide-induced acute lung injury in rats. BMC Physiol. 16, 7. https://doi.org/10.1186/s12899-016-0027-y.

Liang, W., Chow, M.Y.T., Chow, S.F., Chan, H.K., Kwok, P.C.L., Lam, J.K.W., 2018. Using two-fluid nozzle for spray freeze drying to produce porous powder formulation of naked siRNA for inhalation. Int. J. Pharm. 552, 67–75. https://doi.org/10.1016/J.IJPHARM.2018.09.045.

Lock, J.Y., Carlson, T.L., Carrier, R.L., 2018. Mucus models to evaluate the diffusion of drugs and particles. Adv. Drug Deliv. Rev. https://doi.org/10.1016/j.addr.2017.11.001.

Masnabadi, N., Mohammad, H., Ghasemi, Mostafa, Beyki, H., Sadeghinia, Mohammad, 2017. Oxidative dimerization of thiols to disulfide using recyclable magnetic nanoparticles. Res. Chem. Intermed. 43, 1609–1618. https://doi.org/10.1007/s11164-016-2718-1.

Miyata, K., Oba, M., Nakanishi, M., Fukushima, S., Yamasaki, Y., Koyama, H., Nishiyama, N., Kataoka, K., 2008. Polyplexes from poly(aspartamide) bearing 1,2-diaminoethane side chains induce pH-selective, endosomal membrane destabilization with amplified transfection and negligible cytotoxicity. J. Am. Chem. Soc 130, 16287–16294. https://doi.org/10.1021/ja804561g.

Mullings, R.E., Wilson, S.J., Puddicombe, S.M., Lordan, J.L., Bucchieri, F., Djukanović, R., Howarth, P.H., Harper, S., Holgate, S.T., Davies, D.E., 2001. Signal transducer and activator of transcription 6 (STAT-6) expression and function in asthmatic bronchial epithelium. J. Allergy Clin. Immunol. 108, 832–838. https://doi.org/10.1067/mai.2001.119554.

Murgia, X., Loretz, B., Hartwig, O., Hittinger, M., Lehr, C.M., 2018. The role of mucus on drug transport and its potential to affect therapeutic outcomes. Adv. Drug Deliv. Rev. 124, 82–97. https://doi.org/10.1016/J.ADDR.2017.10.009.

Okuda, T., Morishita, M., Mizutani, K., Shibayama, A., Okazaki, M., Okamoto, H., 2018. Development of spray-freeze-dried siRNA/PEI powder for inhalation with high aerosol performance and strong pulmonary gene silencing activity. J. Control Release 279, 99–113. https://doi.org/10.1016/J.JCONREL.2018.04.003.

P.L. Paggiaro, Guida Pocket Per La Gestione E La Prevenzione Dell'asma 2019, Momento Medico S.r.l. 19AK0348 - 07/19.

Park, J., Park, J., Pei, Y., Xu, J., Yeo, Y., 2016. Pharmacokinetics and biodistribution of recently-developed siRNA nanomedicines. Adv. Drug Deliv. Rev. 104, 93–109. https://doi.org/10.1016/j.addr.2015.12.004.

Patel, S., Kim, J., Herrera, M., Mukherjee, A., Kabanov, A.V., Sahay, G., 2019. Brief update on endocytosis of nanomedicines. Adv. Drug Deliv. Rev. 144, 90–111. https://doi.org/10.1016/j.addr.2019.08.004.

Porsio, B., Cusimano, M.G., Schillaci, D., Craparo, E.F., Giammona, G., Cavallaro, G., 2017. Nano into Micro Formulations of Tobramycin for the Treatment of Pseudomonas aeruginosa Infections in Cystic Fibrosis. Biomacromolecules 18, 3924–3935. https://doi.org/10.1021/acs.biomac.7b00945.

Rippmann, J.F., Schnapp, A., Weith, A., Hobbie, S., 2005. Gene silencing with STAT6 specific siRNAs blocks eotaxin release in IL-4/TNFα stimulated human epithelial cells. FEBS Lett. 579, 173–178. https://doi.org/10.1016/j.febslet.2004.11.071.

Ryu, H.J., Jung, H.Y., Park, J.S., Ryu, G.M., Jee, Y.H., Kim, J.J., Moon, S.M., Kim, H.T., Lee, J.Y., Koh, I., Kim, J.W., Jae, K.R., Han, B.G., Kim, H., Park, C.S., Oh, B., Park, C., Lee, J.K., Kimm, K., 2006. Gene-based single nucleotide polymorphisms and linkage disequilibrium patterns of 29 asthma candidate genes in the chromosome 5q31-33 region in Koreans. Int. Arch. Allergy Immunol. 139, 209–216. https://doi.org/10.1159/000091166.

Scherholz, M.L., Schlesinger, N., Androulakis, I.P., 2019. Chronopharmacology of glucocorticoids. Adv. Drug Deliv. Rev. 151–152, 245–261. https://doi.org/10.1016/J.ADDR.2019.02.004.

Segura, T., Hubbell, J.A., 2007. Synthesis and *in vitro* characterization of an ABC triblock copolymer for siRNA delivery. Bioconjug. Chem. 18, 736–745. https://doi.org/10.1021/BC060284Y/ASSET/IMAGES/LARGE/BC060284YF00008.JPEG.

Singh, M.S., Peer, D., 2016. SiRNA delivery: current trends and future perspectives. Ther. Deliv. 7, 51–53. https://doi.org/10.4155/TDE.15.88.

StřÍŽ, I., Mio, T., Adachi, Y., Robbins, R.A., Romberger, D.J., Rennard, S.I., 1999. IL-4 and IL-13 stimulate human bronchial epithelial cells to release IL- 8. Inflammation 23, 545–555. https://doi.org/10.1023/A:1020242523697.

Sulaiman, I., Lim, J.C.W., Soo, H.L., Stanslas, J., 2016. Molecularly targeted therapies for asthma: current development, challenges and potential clinical translation. Pulm. Pharmacol. Ther. 40, 52–68. https://doi.org/10.1016/j.pupt.2016.07.005.

Sun, S., Liang, F., Tang, L., Wu, J., Ma, C., 2017. Microstructural investigation of gas shale in Longmaxi Formation, Lower Silurian, NE Sichuan Basin, China. Energy Explor. Exploit. 35, 406–429. https://doi.org/10.1177/0144598716684304.

Tabeling, C., Herbert, J., Hocke, A.C., Lamb, D.J., Wollin, S.L., Erb, K.J., Boiarina, E., Movassagh, H., Scheffel, J., Doehn, J.M., Hippenstiel, S., Maurer, M., Gounni, A.S., Kuebler, W.M., Suttorp, N., Witzenrath, M., 2017. Spleen tyrosine kinase inhibition blocks airway constriction and protects from Th2-induced airway inflammation and remodeling. Allergy 72, 1061–1072. https://doi.org/10.1111/ALL.13101.

Thommes, M., Kaneko, K., Neimark, A.V., Olivier, J.P., Rodriguez-Reinoso, F., Rouquerol, J., Sing, K.S.W., 2015. Physisorption of gases, with special reference to the evaluation of surface area and pore size distribution (IUPAC Technical Report). Pure Appl. Chem. 87, 1051–1069. https://doi.org/10.1515/PAC-2014-1117/PDF.

Tomita, K., Caramori, G., Ito, K., Sano, H., Lim, S., Oates, T., Cosio, B., Chung, K.F., Tohda, Y., Barnes, P.J., Adcock, I.M., 2012. STAT6 expression in T cells, alveolar macrophages and bronchial biopsies of normal and asthmatic subjects. J. Inflamm. 9, 1–10. https://doi.org/10.1186/1476-9255-9-5 (United Kingdom).

Williams, T.J., Jose, P.J., 2000. Role of eotaxin and related CC chemokines in allergy and asthma. Chem. Immunol. 78, 166–177. https://doi.org/10.1159/000058825.

Ying, S., Humbert, M., Barkans, J., Corrigan, C..J, Pfister, R., Menz, G., Larché, M., Robinson, D.S., Durham, S.R., Kay, A.B., 1997. Expression of IL-4 and IL-5 mRNA and protein product by CD4+ and CD8+ T cells, eosinophils, and mast cells in bronchial biopsies obtained from atopic and nonatopic (intrinsic) asthmatics. J. Immunol. 158, 3539–3544.

Zhu, L., Zhu, Q., Zhang, X., Wang, H., 2013. The correlation analysis of two common polymorphisms in STAT6 gene and the risk of asthma: a meta-analysis. PLOS One 8. https://doi.org/10.1371/journal.pone.0067657.